

Spectrum of heavy baryons in the quark model

T. Yoshida,¹ E.Hiyama,^{2,1,3} A.Hosaka,^{4,3} M. Oka,^{1,3} and K. Sadato^{*4}

¹*Department of Physics, Tokyo Institute of Technology, Meguro 152-8551, Japan*

²*Nishina Center for Accelerator-Based Science, RIKEN, Wako 351-0198, Japan*

³*Advanced Science Research Center, Japan Atomic Energy Agency, Tokai, Ibaraki, 319-1195 Japan*

⁴*Research Center for Nuclear Physics (RCNP), Osaka University, Ibaraki, Osaka 567-0047, Japan*
(Dated: March 6, 2022)

Single- and double- heavy baryons are studied in the constituent quark model. The model Hamiltonian is chosen as a standard one with two exceptions : (1) The color-Coulomb term depend on quark masses, and (2) an antisymmetric LS force is introduced. Model parameters are fixed by the strange baryon spectra, Λ and Σ baryons. The masses of the observed charmed and bottomed baryons are, then, fairly well reproduced. Our focus is on the low-lying negative-parity states, in which the heavy baryons show specific excitation modes reflecting the mass differences of heavy and light quarks. By changing quark masses from the SU(3) limit to the strange quark mass, further to the charm and bottom quark masses, we demonstrate that the spectra change from the SU(3) symmetry patterns to the heavy quark symmetry ones.

I. INTRODUCTION

Recent hadron physics has been stimulated by observations of exotic hadrons with heavy quarks. So-called X, Y, Z mesons contain most likely a hidden heavy quark and antiquark pair, either $\bar{c}c$ or $\bar{b}b$. In addition, they may contain light quark and antiquark pair, thus forming a multiquark configuration near the threshold region of open flavor. For instance, $X(3872), Z_b(10610, 10850)$ are expected to be hadronic molecules of $D\bar{D}^*, B\bar{B}^*$ or $B^*\bar{B}^*$ via strong correlation of quark and antiquark pair [1] [2]. Furthermore, the recently discovered penta-quarks, $P_c(4380)$ and $P_c(4450)$, by LHCb [3] may also have such a structure.

Theoretically, diquark qq correlations may also play an important role, leading to the idea of compact tetraquarks [4] [5]. In fact, the diquark correlations have been considered for long time in many different contexts [6] to explain the mass ordering of light scalar mesons, weak decays of hyperons, missing nucleon resonances, novel phase structure of the quark matter and so on. In QCD, the correlation densities of the two light quarks were measured, having indicated a strong attraction in a so called good diquark pair [7]. In reality, the evidence should be also seen in masses of excited states. Charmed baryons with two light quarks may provide a good opportunity for such a study.

A pioneering work was done some time ago by Copley et al.[8] in a constituent quark model, and later elaborated by Roberts and Pervin [9]. They studied various excited states of charmed and bottomed baryons by solving three quark systems explicitly. Yet a motivation of the present work is to further point out the behavior of various properties of heavy baryons as functions of the heavy quark mass, smoothly interpolating the SU(3) limit of equal quark masses and the heavy quark limit.

Such a study in different flavor regions is useful to systematically understand the nature of spectrum, in particular the roles of the two internal motions when baryons are regarded as three-body systems of quarks. Then the structure information must show up sensitively in various transition amplitudes of decays and productions, which can be studied experimentally as planned at J-PARC and FAIR.

Let us start by briefly showing the essential features of the three quark systems with one heavy quark (Q) of mass m_Q and the two light quarks (q) of equal mass m_q using a non-relativistic quark model with a harmonic oscillator potential for confinement [8].

It is convenient to introduce the Jacobi coordinates, $\lambda = \mathbf{r}_Q - \frac{\mathbf{r}_{q1} + \mathbf{r}_{q2}}{2}$ and $\rho = \mathbf{r}_{q2} - \mathbf{r}_{q1}$, with obvious notations. In the harmonic oscillator potential, the two degrees of freedom decouple and the Hamiltonian can be written simply as a sum the two parts,

$$H = \sum_i \frac{\mathbf{p}_i^2}{2m_i} + \sum_{i<j} \frac{k}{2} |\mathbf{r}_i - \mathbf{r}_j|^2 \\ = \frac{\mathbf{p}_\rho^2}{2m_\rho} + \frac{\mathbf{p}_\lambda^2}{2m_\lambda} + \frac{m_\rho \omega_\rho^2}{2} \rho^2 + \frac{m_\lambda \omega_\lambda^2}{2} \lambda^2, \quad (1)$$

where, m_ρ and m_λ denote the reduced masses

$$m_\rho = \frac{m_q}{2}, \quad m_\lambda = \frac{2m_q m_Q}{2m_q + m_Q}. \quad (2)$$

and the oscillator frequencies ω_ρ and ω_λ are given by

$$\omega_\rho = \sqrt{\frac{3k}{2m_\rho}} \quad \omega_\lambda = \sqrt{\frac{2k}{m_\lambda}}. \quad (3)$$

The ratio of the two excited energy is then given by

$$\frac{\omega_\lambda}{\omega_\rho} = \sqrt{\frac{1}{3}(1 + 2m_q/m_Q)} \leq 1. \quad (4)$$

*present address G-search Ltd. Tamachi 108-0022, Japan.

In the SU(3) limit, equal quark masses, $m_q = m_Q$, the λ and ρ modes degenerate, $\omega_\lambda = \omega_\rho$. However, when $m_Q > m_q$, the excited energy of the λ mode is smaller than that of the ρ mode, $\omega_\lambda < \omega_\rho$ (See Fig.1). Thus, we expect that in the heavy quark sector, the λ excitation modes become dominant for low lying states of singly heavy quark baryons. In contrast, when $m_Q < m_q$, which corresponds to doubly heavy-quark baryons, we have $\omega_\lambda > \omega_\rho$, and therefore, the ρ excitation modes become dominant. It is shown that this feature is rather general for non-relativistic potential models except for the case when the Coulomb type potential of $1/r$ dominates the binding.

One important symmetry structure realized in the heavy quark hadrons is the heavy quark spin symmetry (HQS) [10]. In the heavy quark limit, the interactions which depend on the spin of the heavy quark disappear. Thus, in a single-heavy hadron the heavy quark spin \mathbf{s}_Q is conserved, i.e., $[H, \mathbf{s}_Q] = 0$, and, with the conservation of the total angular momentum \mathbf{J} , one sees that $\mathbf{j} \equiv \mathbf{J} - \mathbf{s}_Q$, angular momentum carried by the light quarks (including all the orbital angular momenta) is also conserved. We will call j light-spin-component. Consequently, two states whose quantum number are $J = j + 1/2$ and $J = j - 1/2$ will be degenerate. They form a heavy quark spin doublet, except for $j = 0$, which yields HQS singlet. A simple example of HQS doublet is the pair of $\Sigma_Q(1/2^+)$ and $\Sigma_Q(3/2^+)$. The mass differences $\Sigma_s(3/2^+) - \Sigma_s(1/2^+) = 174$ MeV, $\Sigma_c(3/2^+) - \Sigma_c(1/2^+) = 63$ MeV and $\Sigma_b(3/2^+) - \Sigma_b(1/2^+) = 22$ MeV decrease as m_Q becomes large.

We organize this paper as follows. In section II, we present our formulation of the non-relativistic constituent quark model. The Hamiltonian and the quark interaction are introduced in section II.A; we employ a linear potential for quark confinement supplemented by spin-spin, tensor and spin-orbit (LS) forces. The anti-symmetric LS force is also needed to guarantee the heavy quark symmetry. In II.B, the Gaussian expansion method is introduced to solve the three-quark system. When the heavy quark mass is varied from $m_Q = m_q$ to $m_Q \rightarrow \infty$, then the symmetry of the spectrum changes from the SU(3) to the heavy quark spin symmetry. In section II.C, the relation of the two symmetry limits and mixings of the two internal excitation modes are discussed. The results of the present work are presented in section III. The results of single-heavy baryons and those of double-heavy baryons are discussed in III.A and III.D, respectively. The properties of the λ and ρ modes are discussed in III.C in detail. In III.D, the heavy quark limit is investigated. Finally, a summary is given in Section IV.

II. FORMALISM

A. Hamiltonian

In this subsection, we discuss our model Hamiltonian in detail. In the non-relativistic quark model, baryons are formed by three valence (constituent) quarks. They are confined by a confining potential and interact with each other by residual two-body interactions. Their internal motions are then described by the two spatial variables $\boldsymbol{\rho}$ and $\boldsymbol{\lambda}$. In other models of baryons, non-quark degrees of freedom are considered such as constituent gluons and confining fields. Their signals in baryon excitations are, however, not yet confirmed in experiments, and are expected to lie at higher energies than the low lying quark excitation modes. Empirically these justify the applicability of the quark model, especially for low lying excitation modes.

Thus our Hamiltonian is written as

$$H = K + V_{\text{con}} + V_{\text{short}}, \quad (5)$$

where the kinetic energy, K , the confinement potential, V_{con} , and the short range interaction, V_{short} , are given as

$$K = \sum_i \left(m_i + \frac{\mathbf{p}_i^2}{2m_i} \right) - K_G, \quad (6)$$

$$V_{\text{con}} = \sum_{i < j} \frac{br_{ij}}{2} + C \quad (7)$$

$$\begin{aligned} V_{\text{short}} = & \sum_{i < j} \left[-\frac{2\alpha^{\text{Coul}}}{3r_{ij}} + \frac{16\pi\alpha^{\text{ss}}}{9m_i m_j} \mathbf{s}_i \cdot \mathbf{s}_j \frac{\Lambda^2}{4\pi r_{ij}} \exp(-\Lambda r_{ij}) \right. \\ & + \frac{\alpha^{\text{so}}(1 - \exp(-\Lambda r_{ij}))^2}{3r_{ij}^3} \\ & \times \left[\left(\frac{1}{m_i^2} + \frac{1}{m_j^2} + 4\frac{1}{m_i m_j} \right) \mathbf{L}_{ij} \cdot (\mathbf{s}_i + \mathbf{s}_j) \right. \\ & \left. \left. + \left(\frac{1}{m_i^2} - \frac{1}{m_j^2} \right) \mathbf{L}_{ij} \cdot (\mathbf{s}_i - \mathbf{s}_j) \right] \right. \\ & \left. + \frac{2\alpha^{\text{ten}}(1 - \exp(-\Lambda r_{ij}))^2}{3m_i m_j r_{ij}^3} \left(\frac{3(\mathbf{s}_i \cdot \mathbf{r}_{ij})(\mathbf{s}_j \cdot \mathbf{r}_{ij})}{r_{ij}^2} \right. \right. \\ & \left. \left. - \mathbf{s}_i \cdot \mathbf{s}_j \right) \right]. \quad (8) \end{aligned}$$

In Eq.(6), m_i is the constituent quark mass of the i -th quark, and the center of mass energy, K_G , is subtracted so that the kinetic energy consists only of the ρ and λ -kinetic energies. In Eq.(7), we employ the linear confinement potential with the b parameter corresponding to the string tension and $\mathbf{r}_{ij} = \mathbf{r}_i - \mathbf{r}_j$ is the relative coordinate. In Eq.(8), $\mathbf{L}_{ij} = (\mathbf{r}_i - \mathbf{r}_j) \times (m_j \mathbf{p}_i - m_i \mathbf{p}_j) / (m_i + m_j)$ is the relative orbital angular momentum and $\mathbf{s}_i (= \boldsymbol{\sigma}_i / 2)$

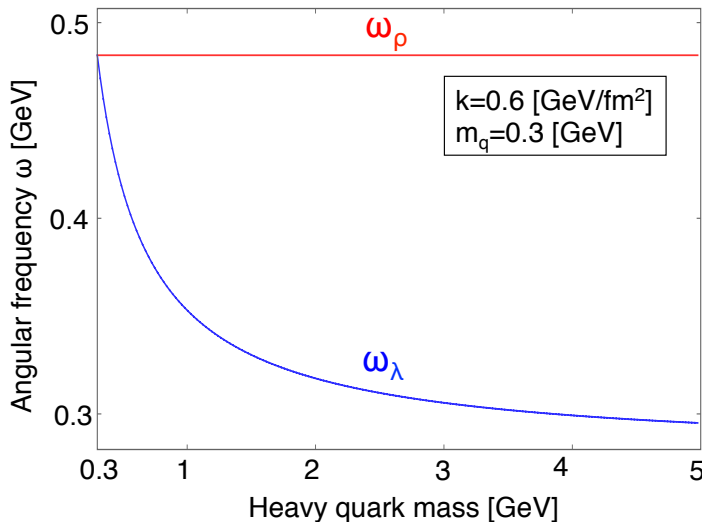


FIG. 1: Heavy quark mass dependence of excited energies of the λ -mode (red solid line) and the ρ -mode (blue solid line) in Eq.(1)

is the spin operators of the i -th quark. The components of Eq.(8) are inferred by the one-gluon-exchange (OGE), which requires only one coupling constant common to the four terms. Practically, however, they may have different origins other than the OGE, and therefore, we treat the four coupling strengths, α^{Coul} , α^{ss} , α^{so} and α^{ten} as independent parameters for better description of baryon masses.

In order to guarantee the heavy quark symmetry, we introduce anti-symmetric LS force (ALS). The terms dependent on the heavy quark spin \mathbf{s}_Q of the V_{SLS} and V_{ALS} in a single-heavy baryon are given by

$$V_{\text{SLS}} \rightarrow \sum_{i=1,2} \frac{\alpha^{\text{so}}(1 - \exp(-\Lambda r_{iQ}))^2}{3r_{iQ}^3} \times \left(\frac{1}{m_i^2} + \frac{1}{m_Q^2} + \frac{4}{m_i m_Q} \right) \mathbf{L}_{iQ} \cdot \mathbf{s}_Q \quad (9)$$

$$V_{\text{ALS}} \rightarrow \sum_{i=1,2} \frac{\alpha^{\text{so}}(1 - \exp(-\Lambda r_{iQ}))^2}{3r_{iQ}^3} \quad (10)$$

$$\times \left(\frac{1}{m_i^2} - \frac{1}{m_Q^2} \right) \mathbf{L}_{iQ} \cdot (-\mathbf{s}_Q) \quad (11)$$

where we choose $i = 3$ for the heavy quark. Then by summing the parts from SLS and ALS, the $\mathbf{L}_Q \cdot \mathbf{s}_Q$ is always proportional to $1/m_Q$ or higher. Thus the \mathbf{s}_Q dependence disappears in the $m_Q \rightarrow \infty$ limit, and the heavy quark symmetry is guaranteed.

Recently, it was suggested by a Lattice QCD

calculation[11] that the strength, α^{Coul} , of the color Coulomb force depends significantly on the quark mass. In our study, we therefore assume that α^{Coul} for the $i - j$ pair of quarks depends on the reduced mass, $\mu_{ij} = \frac{m_i m_j}{m_i + m_j}$, as follows,

$$\alpha^{\text{Coul}} = \frac{K}{\mu_{ij}}. \quad (12)$$

We summarize 10 parameters in the Hamiltonian employed here in TABLE I. The parameters are determined from experimental data of the strange baryon spectrum (See TABLE II). First, we switch off the LS and tensor force to determine the parameters C , α_{ss} , m_q , m_s and Λ , K from the positive parity state. Then, we determine α^{so} , b from negative parity states. The details how to determine the parameters are as follows.

- The constant term C

In the constituent quark models, we can predict mass differences between different states, but the absolute values can not be determined. In our work, we introduce the constant C to reproduce the ground state of $\Lambda(1115)$ and we assume that the constant C is independent of the constituent quark mass. Namely, we use the same value for the charmed baryons.

- Spin-spin term

The spin-spin term in the hamiltonian is responsible for the splitting among Λ , Σ and Σ^* . This term depends on α^{ss} , m_q , m_s and Λ . Because we have four parameters for three states to be fitted, we fix $m_q = 300$ MeV which is the standard value suggested from the magnetic moment of the baryon in the constituent quark model and then we determine the other parameters to reproduce the masses of Λ , Σ , Σ^* .

- The parameter K

In our calculation, we introduce α^{Coul} as a quark mass dependent form as given by Eq (12). Thus, the Coulomb force can contribute to the mass splitting between the ground states of $\Lambda_s(\Sigma_s)$, Ξ_{ss} , Ω_{sss} . This force also contributes to the mass differences between the ground state and the excited states. We determine the parameter K to reproduce $\Xi(1/2^+)$ and the mass difference between the ground state and the excited states.

- The linear confinement b

Our emphasis in the present study is on the P wave states. The parameters which mainly determine the mass differences are b and K . K is determined from $\Xi(1/2^+)$ as mentioned above and we determine the parameter b to reproduce the splitting between ground state and P-wave state.

- The spin-orbit coupling α^{so}

The strength α^{so} of the spin-orbit force may be determined by the splitting of the P-wave baryons, such as $\Lambda(1/2^-)$ and $\Lambda(3/2^-)$. However, we do not use the lowest $\Lambda(1/2^-)$, $=\Lambda(1405)$, because various recent studies on the $\Lambda(1405)$ resonance suggests that this is not simply a pure three-quark state, but rather a $N\bar{K}$ molecular-like state. Therefore, we determine the parameter α^{so} to reproduce the splitting between the second $\Lambda(1/2^-)$ and $\Lambda(3/2^-)$, namely $\Lambda(1670)$ and $\Lambda(1690)$. Thus, as expected, α_{so} becomes very small, much smaller than α_{ss} . If the spin-spin and LS forces come only from the OGE, then their values are not consistent. However, other sources of quark interactions including the relativistic correlations to the confinement and instanton induced interaction(III) may contribute also the LS interaction shown[12] that the LS force from OGE and III are opposite. Then the discrepancy between α^{ss} and α^{so} can be explained.

- The strength α^{ten}

The tensor force in the hamiltonian contributes mainly to the positive parity $\Sigma(1/2^+)$, $\Sigma(3/2^+)$

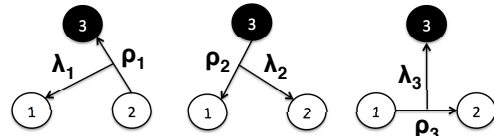


FIG. 2: Jacobi coordinates for the three body system. We place the heavy quark as the 3rd particle in the case of single-heavy baryons, while the 1st and 2nd particles are heavy quarks in double-heavy baryons.

and the lowest negative states. It has been known that the tensor force is weak and does not contribute much except for generating mixings of $S = 1/2$ and $3/2$ states. We choose α^{ten} equal to α^{so}

- Charm and bottom quark mass, m_c, m_b

We fit the charm quark mass m_c (bottom quark mass m_b) to the ground state of Λ_c (Λ_b). These values contribute to the mass splittings as well as the absolute values, but once we determine the other parameters in the strange sector, m_c and m_b are determined uniquely.

From Table II, we find that our results reproduce most of the known strange baryon masses, except for the second $J^P = 1/2^+$ state and the first $J^P = 1/2^-$. It is well known that the Roper resonance $N(1440)$, the second $J^P = 1/2^+$ state, is lighter than lowest $J^P = 1/2^-$ state, which is incompatible with the quark model predictions. Similarly, in the strange sector, the Roper-like states $\Lambda(1600)$ and $\Sigma(1660)$, are predicted at higher masses than experiment. The origin of these discrepancies may reside outside the simple three quark picture of the baryons in the quark model. We therefore omit these states from the fitting in the present analysis.

B. Baryon wave-function

We here consider three quark systems (TABLE.III) with one heavy quark, $Q = (c \text{ or } b)$, with two or three heavy quarks with the same flavor, i.e., $QQ = (cc \text{ or } bb)$ and $QQQ = (ccc \text{ or } bbb)$. The remaining quarks are u , d or s . We classify the baryons according to the number of heavy quarks, and the strangeness, \mathcal{S} and the total isospin, T . The last column of the TABLE.III shows the isospin wave function where $\eta_0 = 1$.

In expressing three-quark wave functions, we introduce three sets of Jacobi coordinates, which we call channels (Fig. 2). The Jacobi coordinates in each channel c ($c =$

m_q	m_s	m_c	m_b	b	K	α^{ss}	$\alpha^{so}(=\alpha^{\text{ten}})$	C	Λ
[MeV]	[MeV]	[MeV]	[MeV]	[GeV ²]	[MeV]			[MeV]	[fm ⁻¹]
300	510	1750	5112	0.165	90	1.2	0.077	-1139	3.5

TABLE I: Parameters in the Hamiltonian. We determine m_q , m_s , b , K , α^{ss} and Λ to reproduce strange baryons and m_c and m_b are determined from the ground state of Λ_c and Λ_b .

(a) Λ_s			(b) Σ_s			(c) Ξ_{ss}			
J^P	Theory	Exp.	J^P	Theory	Exp.	J^P	Theory	Exp.	
	[MeV]	[MeV]		[MeV]	[MeV]		[MeV]	[MeV]	
$\frac{1}{2}^+$	1116	1116	$\frac{1}{2}^+$	1197	1192	$\frac{1}{2}^+$	1325	1314	
	1799	1560-1700		1895	1630-1690		1962		
	1922	1750-1850		2016			2131		
$\frac{3}{2}^+$	1882	1850-1910	$\frac{3}{2}^+$	1391	1385	$\frac{3}{2}^+$	1525	1530	
	2030			2004			2034		
	2100			2028			2115		
$\frac{5}{2}^+$	1891	1815-1825	$\frac{5}{2}^+$	2012	1900-1935	$\frac{5}{2}^+$	2040		
	2045	2090-2140		2085			2166		
	2143			2091			2211		
$\frac{1}{2}^-$	1526	1405	$\frac{1}{2}^-$	1654	(≈ 1620)	$\frac{1}{2}^-$	1778		
	1665	1660-1680		1734	1730-1800		1875		
	1777	1720-1850		1751			1910		
$\frac{3}{2}^-$	1537	1520	$\frac{3}{2}^-$	1660	1665-1685	$\frac{3}{2}^-$	1782	1820	
	1685	1685-1695		1755	1900-1950		1877		
	1810			1760			1920		
$\frac{5}{2}^-$	1814	1810-1830	$\frac{5}{2}^-$	1762	1770-1780	$\frac{5}{2}^-$	1933		
	2394			2324			2460		
	2448			2427			2518		

TABLE II: Calculated energy spectra and corresponding experimental data of Λ_s, Σ_s and Ξ_{ss} . We take the 3-star and 4-star resonances in PDG except for the first $1/2^-$ state of Σ_s which has only two stars

1, 2, 3) are defined as

$$\lambda_c = \mathbf{r}_k - \frac{m_i \mathbf{r}_i + m_j \mathbf{r}_j}{m_i + m_j}, \quad (13)$$

$$\rho_c = \mathbf{r}_j - \mathbf{r}_i, \quad (14)$$

where (i, j, k) are given by Table IV.

The total wave function is given as a superposition of the channel wave functions as

$$\Phi_{\text{total}}^{JM} = \sum_{c\alpha} C_{c,\alpha} \Phi_{JM,\alpha}^{(c)}(\rho_c, \lambda_c), \quad (15)$$

where the index α represents $\{s, S, \ell, L, I, n, N\}$. Here s is the spin of the (i, j) quark pair, S is the total spin, ℓ and L are the orbital angular momentum for the coordinate ρ and λ , respectively, and I is the total orbital angular momentum. The coupling scheme of the spin

and angular momenta is as

$$\mathbf{s} = \mathbf{s}_i + \mathbf{s}_j; \quad \mathbf{s} + \mathbf{s}_k = \mathbf{S}; \quad \ell + \mathbf{L} = \mathbf{I}; \quad \mathbf{S} + \mathbf{I} = \mathbf{J}. \quad (16)$$

The wave function for channel c is given by

$$\Phi_{JM}^{(c)}(\rho_c, \lambda_c) = \phi_c \otimes [X_{S,s}^{(c)} \otimes \Phi_{\ell,L,I}^{(c)}]_{JM} \otimes H_{T,t}^{(c)}, \quad (17)$$

where the color wave function, ϕ_c , the spin wave function, X_S , the orbital wave function, Φ_I , and the isospin wave function, H_T , are given by

$$\phi_c = \frac{1}{\sqrt{6}}(rgb - rbg + gbr - grb + brg - bgr) \quad (18)$$

$$X_{S,s}^{(c)} = [[\chi_{1/2}(i)\chi_{1/2}(j)]_s \chi_{1/2}(k)]_S \quad (19)$$

Heavy baryons	Isospin	Strangeness	isospin wave function
	\mathcal{S}	T	
$\Lambda_Q = [qq]_{T=0}Q$	0	0	$[[\eta_{1/2}\eta_{1/2}]_{t=0}\eta_0]_{T=0}$
$\Sigma_Q = [qq]_{T=1}Q$	0	1	$[[\eta_{1/2}\eta_{1/2}]_{t=1}\eta_{1/2}]_{T=1}$
$\Xi_Q = sqQ$	-1	1/2	$[[\eta_0\eta_{1/2}]_{t=1/2}\eta_0]_{T=1/2}$
$\Omega_Q = ssQ$	-2	0	1
$\Xi_{QQ} = QQq$	0	1/2	$[[\eta_0\eta_0]_{t=0}\eta_{1/2}]_{T=1/2}$
$\Omega_{QQ} = QQs$	-1	0	1
$\Omega_{QQQ} = QQQ$	0	0	1

TABLE III: Heavy baryons and their flavor contents. We use the isopin classification so that q stands collectively for the u and d quarks. Q denotes a c or b quark. We do not consider mixing of c and b

channel	i	j	k
1	2	3	1
2	3	1	2
3	1	2	3

TABLE IV: The quark assignments (i,j,k) for the Jacobi channels.

$$H_{T,t}^{(c)} = [[\eta_{\tau_i}(i)\eta_{\tau_j}(j)]_t \eta_{\tau_k}(k)]_T \quad (20)$$

$$\Phi_{\ell,L,I}^{(c)} = [\phi_{\ell}^{(c)}(\boldsymbol{\rho}_c)\phi_L^{(c)}(\boldsymbol{\lambda}_c)]_I \quad (21)$$

$$\phi_{\ell}^{(c)}(\boldsymbol{\rho}_c) = N_{n\ell}\rho_c^{\ell}e^{-\beta_n\rho_c^2}Y_{\ell m}(\hat{\boldsymbol{\rho}}_c) \quad (22)$$

$$\phi_L^{(c)}(\boldsymbol{\lambda}_c) = N_{NL}\lambda_c^L e^{-\gamma_N\lambda_c^2}Y_{LM}(\hat{\boldsymbol{\lambda}}_c). \quad (23)$$

In Eq. (18), r, g, b denote the color of the quark, and the color-singlet wave function is totally anti-symmetric. In Eq.(19), $\chi_{1/2}$ is the spin wave function of the quark, while η_{τ} in Eq.(20) is the isospin wave function with τ defined by

$$\tau = \begin{cases} 1/2 & \text{for } u, d \\ 0 & \text{for } s, c, b \end{cases} \quad (24)$$

We consider the quark antisymmetrization for the light quarks, u and d , and the heavy quarks, s, c, b , separately. Then for single-heavy baryons, antisymmetrization is applied only to the light quarks. As the color wave function is always totally anti-symmetric, the spin, isospin and the orbital angular momentum in the channel (3) should satisfy

$$\ell + s + t = \text{even} \quad \text{for } \Lambda_Q, \Sigma_Q \quad (25)$$

where ℓ, s, t are the orbital angular momentum, total spin and isospin of the two light quarks. Similarly, the heavy quarks are antisymmetrized in the double-heavy baryons as

$$\ell + s + 1 = \text{even} \quad \text{for } \Xi_{QQ}, \Omega_Q, \Omega_{QQ} \quad (26)$$

where ℓ, s, t are the corresponding ones for the heavy quarks. Considering the antisymmetrization and the combinations of the angular momenta, we obtain possible assignments of the angular momenta for the low-lying $\Lambda_Q(1/2^+)$ in Table V, where we take all the combinations satisfying $\ell + L \leq 2$.

In solving the Schrödinger equation, we use the Gaussian expansion method [13], where the orbital wave functions are expanded, in Eqs. (22) and (23), by Gaussian functions with the range parameters, β_n and γ_N , chosen as:

$$\beta_n = 1/r_n^2, \quad r_n = r_1 a^{n-1} \quad (n = 1, \dots, n_{\max}), \quad (27)$$

$$\gamma_N = 1/R_N^2, \quad R_N = R_1 b^{N-1} \quad (N = 1, \dots, N_{\max}). \quad (28)$$

In Eqs (22) and (23), $N_{n\ell}(N_{NL})$ denotes the normalization constant of the Gaussian basis. The coefficients $C_{c,\alpha}$ of the variational wave function, Eq.(15), are determined by the Rayleigh-Ritz variational principle. In order to check that the energy converges to the required precision, we change the number of bases and plot the eigen-energy of the lowest lying $\Lambda_c(3/2^-)$ in Fig.3. The filled points are the results from the calculation only using the channel 3, while the open circles are the results from the three channel calculation (Fig.2). One sees that when we take only one channel, the convergence is slow and has not yet reached the required precision at $N_{\max} = n_{\max} = 10$.

C. Heavy quark limit

One of the aims of this paper is to see how the heavy baryon spectrum changes when the heavy quark mass m_Q

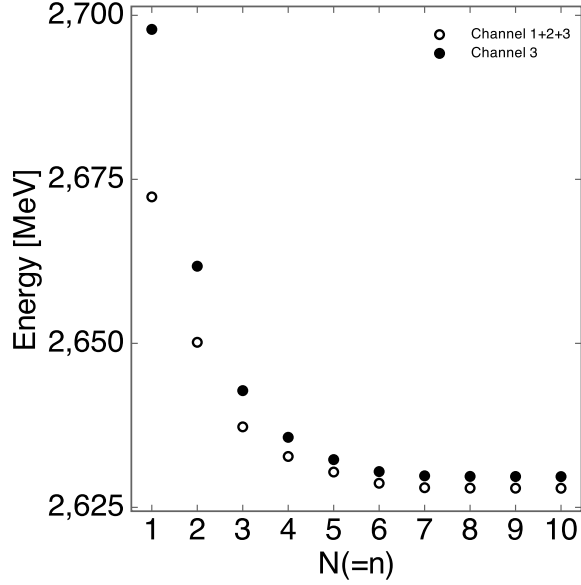


FIG. 3: Convergence of the energy of the lowest $\Lambda_c(3/2^-)$ for increasing the number of bases functions.

channel	ℓ	L	I	s	S
3	0	0	0	0	1/2
3	1	1	0	1	1/2
3	1	1	1	1	1/2
3	1	1	1	1	3/2
3	1	1	2	1	3/2

TABLE V: Combinations of the spin and orbital angular momenta in channel 3 of the low-lying $\Lambda(1/2^+)$. In our study, we restrict the total angular momentum up to 2, $\ell + L = 0, 2$.

changes. Two limits are important: the SU(3) limit with $m_Q = m_q$, and the heavy quark (HQ) limit, $m_Q \rightarrow \infty$.

In the limit $m_Q \rightarrow m_q$, the spectrum is classified by the SU(3) representations. For instance, the lowest P -wave baryons are expected to belong to the SU(6) 70-dimensional representation, which contains ${}^2\mathbf{1}$, ${}^2\mathbf{8}$, ${}^4\mathbf{8}$, and ${}^2\mathbf{10}$. Here the upper index number is the spin multiplicity and the bold number represents the SU(3) multiplicity. On the other hand, in the HQ limit, $m_Q \rightarrow \infty$, as we have discussed in sect.I, the P -wave baryons are better classified by the ρ - and λ -excitation modes (Fig.4). Here we derive relations between the two pictures.

Let us consider single-heavy Λ_Q and Σ_Q baryons. We put the heavy quark Q as the 3rd quark. Then the orbital-spin wave functions of Λ_Q and Σ_Q in the SU(3)

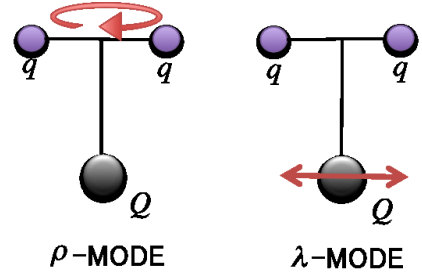


FIG. 4: The ρ - and λ -modes excitations of the single-heavy baryon.

limit are given by

$$\Psi(\Lambda_Q; {}^2\mathbf{1}) = \frac{1}{\sqrt{2}}(X_{1/2,1}\Phi_{1,0,1} - X_{1/2,0}\Phi_{1,1,0}). \quad (29)$$

$$\Psi(\Lambda_Q; {}^2\mathbf{8}) = \frac{1}{\sqrt{2}}(X_{1/2,1}\Phi_{1,0,1} + X_{1/2,0}\Phi_{1,1,0}) \quad (30)$$

$$\Psi(\Lambda_Q; {}^4\mathbf{8}) = X_{3/2,1}\Phi_{1,0,1} \quad (31)$$

and

$$\Psi(\Sigma_Q; {}^2\mathbf{10}) = \frac{1}{\sqrt{2}}(X_{1/2,1}\Phi_{1,1,0} + X_{1/2,0}\Phi_{1,0,1}) \quad (32)$$

$$\Psi(\Sigma_Q; {}^2\mathbf{8}) = \frac{1}{\sqrt{2}}(X_{1/2,1}\Phi_{1,1,0} - X_{1/2,0}\Phi_{1,0,1}) \quad (33)$$

$$\Psi(\Sigma_Q; {}^4\mathbf{8}) = X_{3/2,1}\Phi_{1,1,0}. \quad (34)$$

In the SU(3) limit, the ${}^2\mathbf{8}(S = 1/2)$ and ${}^4\mathbf{8}(S = 3/2)$ can be mixed with the spin-spin/spin-orbit forces (If we further argue SU(6), they do not mix). For $m_q < m_Q$, $\Psi(\Lambda_Q; {}^2\mathbf{1})$ and $\Psi(\Lambda_Q; {}^2\mathbf{8})$ may mix with each other and in the large m_Q limit, they are reduced to the λ -mode, $\Phi_{1,1,0}$, and the ρ -mode, $\Phi_{1,0,1}$, excitations. Representing the $\lambda(\rho)$ -mode with the total spin S by ${}^{2S+1}\lambda({}^{2S+1}\rho)$, we obtain

$$\begin{aligned} \Psi(\Lambda_Q; {}^2\lambda) &= X_{1/2,0}\Phi_{1,1,0} \\ &= \frac{1}{\sqrt{2}}(\Psi(\Lambda_Q; {}^2\mathbf{8}) - \Psi(\Lambda_Q; {}^2\mathbf{1})) \end{aligned} \quad (35)$$

$$\begin{aligned} \Psi(\Lambda_Q; {}^2\rho) &= X_{1/2,1}\Phi_{1,0,1} \\ &= \frac{1}{\sqrt{2}}(\Psi(\Lambda_Q; {}^2\mathbf{8}) + \Psi(\Lambda_Q; {}^2\mathbf{1})) \end{aligned} \quad (36)$$

$$\Psi(\Lambda_Q; {}^4\rho) = X_{3/2,1}\Phi_{1,0,1} = \Psi(\Lambda_Q; {}^4\mathbf{8}). \quad (37)$$

for the Λ_Q baryons and

$$\begin{aligned}\Psi(\Sigma_Q; ^2\lambda) &= X_{1/2,1}\Phi_{1,1,0} \\ &= \frac{1}{\sqrt{2}}(\Psi(\Sigma_Q; ^2\mathbf{10}) + \Psi(\Sigma_Q; ^2\mathbf{8}))\end{aligned}\quad (38)$$

$$\begin{aligned}\Psi(\Sigma_Q; ^2\rho) &= X_{1/2,0}\Phi_{1,0,1} \\ &= \frac{1}{\sqrt{2}}(\Psi(\Sigma_Q; ^2\mathbf{10}) - \Psi(\Sigma_Q; ^2\mathbf{8}))\end{aligned}\quad (39)$$

$$\Psi(\Sigma_Q; ^4\lambda) = X_{3/2,1}\Phi_{1,1,0} = \Psi(\Sigma_Q; ^4\mathbf{8}),\quad (40)$$

for the Σ_Q baryons.

Generally, the λ -modes appear lower in energy than the ρ -modes and they do not mix with each other in the heavy quark limit. The two states which are in the same mode but have different spin, ($\Lambda_Q; ^2\rho$, $\Lambda_Q; ^4\rho$ and $\Sigma_Q; ^2\lambda$, $\Sigma_Q; ^4\lambda$) may mix even in the heavy quark limit, because the light quark spin-spin force is still alive in this limit. For intermediate heavy quark masses, all these states may mix and the wave functions of energy eigenstates show how the mixings change as the heavy quark mass increases.

A similar analysis can be done for other heavy quark baryons. We tabulate, in Table VI, the λ - and ρ -modes classification of the P -wave heavy quark baryons and their quantum numbers in the Jacobi coordinate channel 3.

In the heavy quark limit, $m_Q \rightarrow \infty$, HQS symmetry becomes exact, where the spin degeneracy of $J = j \pm 1/2$ appears. In this limit, the light component $\mathbf{j} = \mathbf{J} - \mathbf{s}_Q$ and the heavy quark spin \mathbf{s}_Q are conserved independently, $[H, \mathbf{s}_Q] = 0 \rightarrow [H, \mathbf{J} - \mathbf{s}_Q] = [H, \mathbf{j}] = 0$. The basis in which \mathbf{j} becomes diagonal can be written in terms of the Jacobi-coordinate basis states Eq.(17) for the channel $c = 3$ as

$$\begin{aligned}\Psi(qqQ; j; J) &= [[\chi_{1/2}(q)\chi_{1/2}(q)]_s \Phi_{\ell LI}]_j \chi_{1/2}(Q)]_J \\ &= \sum_S (-)^{(s+S+1/2)} \sqrt{(2S+1)(2j+1)} \\ &\quad \times \left\{ \begin{array}{ccc} 1/2 & s & S \\ I & J & j \end{array} \right\} [X_{S,s} \otimes \Phi_{\ell LI}]_J\end{aligned}\quad (41)$$

III. RESULTS AND DISCUSSION

A. Energy spectra of single-heavy systems

We first discuss energy spectra of the single-charmed baryons, Λ_c , Σ_c and Ω_c . The energies of the charmed baryons are listed in Table VII and are illustrated in Fig 5. The mass of the lowest Λ_c is used to fix the charm quark mass m_c . The energy differences among the lowest $\Lambda_c(1/2^+)$, $\Sigma_c(1/2^+)$, $\Sigma_c^*(3/2^+)$ are given by $\Sigma_c(1/2^+) - \Lambda_c(1/2^+) = 175$ MeV (exp. 170 MeV), $\Sigma_c^*(3/2^+) - \Sigma_c(1/2^+) = 71$ MeV (exp. 65 MeV), which agree very well to the experimental data. The mass of the

other single-charmed baryons are also well reproduced within 50 MeV deviation.

There are two observed states, $\Lambda_c(2940)$ and $\Sigma_c(2800)$, whose spin and parity have not been assigned. The present calculation indicates that $\Lambda_c(2940)$ can be assigned to one of the following states, $3/2_1^+$ (2920MeV), $5/2_1^-$ (2960MeV), $1/2_2^-$ (2890MeV), $1/2_3^-$ (2933MeV), $3/2_2^-$ (2917MeV), and $3/2_3^-$ (2956MeV), while $\Sigma_c(2800)$ may be assigned to one of $1/2_1^-$ (2802MeV), $3/2_1^-$ (2807MeV), $1/2_2^-$ (2826MeV), $3/2_2^-$ (2837MeV) and $5/2_1^-$ (2839MeV). Here, J_n^P denotes the n -th J^P state. Further experimental information, such as decay branching ratios and production rates, will be necessary to determine the quantum numbers of these states.

For $S = -2$ baryons, the lowest states of $\Omega_c(1/2^+)$ and $\Omega_c(3/2^+)$ have been experimentally observed. We underestimate the mass difference between them by about 20 MeV.

The masses of the single-bottom baryons are listed in Table VIII and illustrated in Fig 6. The ground state Λ_b is fitted to the experimental data of Particle Data Group. The mass differences among Λ_b , Σ_b , and Σ_b^* are $\Sigma_b(1/2^+) - \Lambda_b(1/2^+) = 188$ MeV, $\Sigma_b^*(3/2^+) - \Sigma_b(1/2^+) = 21$ MeV experimentally, while our calculation gives $\Sigma_b(1/2^+) - \Lambda_b(1/2^+) = 195$ MeV, and $\Sigma_b^*(3/2^+) - \Sigma_b(1/2^+) = 22$ MeV. Thus, we find that the low lying positive-parity states are reproduced within 10 MeV deviation.

The negative parity Λ_b states, $\Lambda_b(5912)$ and $\Lambda_b(5920)$, have been discovered recently. Their mass difference is about 8 MeV in experiment while it is 1 MeV in our prediction. For $S = -2$ bottom baryons, $\Omega_b(1/2^+)$, our estimate of the mass is 6076 MeV, which is higher than the experimental value, 6015 MeV.

B. Energy spectra of double-heavy baryon systems

TABLE IX, X and Figs.7 and 8 show the calculated energy spectra and experimental data for double-heavy baryons. Lattice QCD [14] [15] and quark models [9] [16] predicted the masses of double-heavy baryons and variations among the model calculations are large, compared to those in the single-heavy baryons.

The calculated mass of the lowest Ξ_{cc} state is 3685 MeV, which is much higher than the experimental observations by SELEX[17], 3519 MeV. However, the other experimental searches by BARBAR[18], Belle[19] and LHCb[20], could not confirm this state. Our prediction is consistent with the recent lattice result as well as the other quark model calculations.

We predict that the lowest Ξ_{bb} state is $\Xi_{bb}(\frac{1}{2}^+) = 10314$ MeV followed by $\Xi_{bb}(\frac{3}{2}^+) = 10339$ MeV.

flavor	ℓ	L	I	s	S	mode	J
Λ_Q	0	1	1	0	1/2	$^2\lambda$	$1/2^-, 3/2^-$
	1	0	1	1	1/2	$^2\rho$	$1/2^-, 3/2^-$
	1	0	1	1	3/2	$^4\rho$	$1/2^-, 3/2^-, 5/2^-$
Σ_Q	0	1	1	1	1/2	$^2\lambda$	$1/2^-, 3/2^-$
	0	1	1	1	3/2	$^4\lambda$	$1/2^-, 3/2^-, 5/2^-$
	1	0	1	0	1/2	$^2\rho$	$1/2^-, 3/2^-$
Ξ_Q	0	1	1	0	1/2	$^2\lambda$	$1/2^-, 3/2^-$
	1	0	1	1	1/2	$^2\rho$	$1/2^-, 3/2^-$
	1	0	1	1	3/2	$^4\rho$	$1/2^-, 3/2^-, 5/2^-$
	0	1	1	1	1/2	$^2\lambda$	$1/2^-, 3/2^-$
	0	1	1	1	3/2	$^4\lambda$	$1/2^-, 3/2^-, 5/2^-$
	1	0	1	0	1/2	$^2\rho$	$1/2^-, 3/2^-$
Ξ_{QQ}	0	1	1	1	1/2	$^2\lambda$	$1/2^-, 3/2^-$
	0	1	1	1	3/2	$^4\lambda$	$1/2^-, 3/2^-, 5/2^-$
	1	0	1	0	1/2	$^2\rho$	$1/2^-, 3/2^-$
Ω_{QQ}	0	1	1	1	1/2	$^2\lambda$	$1/2^-, 3/2^-$
	0	1	1	1	3/2	$^4\lambda$	$1/2^-, 3/2^-, 5/2^-$
	1	0	1	0	1/2	$^2\rho$	$1/2^-, 3/2^-$
Ω_{QQQ}	0	1	1	1	1/2	$^2\lambda$	$1/2^-, 3/2^-$
	1	0	1	0	1/2	$^2\rho$	$1/2^-, 3/2^-$

TABLE VI: The λ - and ρ -mode assignments of the P -wave excitations of Λ_Q , Σ_Q , Ξ_Q , Ξ_{QQ} , Ω_{QQ} and Ω_{QQQ} . The quantum numbers are given in the Jacobi coordinate channel 3.

C. λ mode and ρ mode structures in heavy baryon systems

Now we compare the heavy baryon spectra for the strange sector and the heavier sector (c and b) and clarify the quark dynamics in the heavy baryon. Strange baryons are conventionally analyzed by the $SU(3)_f$ symmetry. When the strange quark is replaced by a heavier quark, c or b , we can study the dynamics of the two light quarks, which may be regarded as a diquark. From this point of view, one sees two distinct excitation modes, λ and ρ modes. The λ -mode state is composed of the $(qq)_{\ell=0}$ diquark with $L=1$ excitation relative to the heavy quark, Q , while the ρ -mode state has an excited diquark $(qq)_{\ell=1}$ in the $L=0$ orbit around Q .

As is discussed in Sec.I, the λ - and ρ -modes are largely mixed in the $SU(3)$ limit in the light quark sector. This mixing is induced mainly by the spin-spin interaction. Because the spin dependent interaction for the heavy quark is weak, the λ - and ρ -modes are well separated for the charm and bottom baryons. Then, each P -wave state is dominated and characterized either by the λ -mode or ρ -mode.

In order to demonstrate these properties quantitatively, we change the heavy quark mass, m_Q , from 300 MeV to 6 GeV and analyze the excitation energies and wave functions. Fig. 9 shows the spectra of Λ_Q and Σ_Q

as functions of m_Q . One sees that the splitting between the 1st and 2nd $1/2^-$ state of Λ_Q increases rapidly from 100 MeV in the $SU(3)$ limit to 300 MeV in the heavy quark limit when m_Q increases. This behavior is due to the λ - ρ splitting as demonstrated by the harmonic oscillator model (in Fig.1). Namely, the lowest state becomes dominated by the λ -mode as m_Q becomes large. This is confirmed in Fig.11, where the λ - and ρ -mode probabilities of the lowest $1/2^-$ state are plotted as functions of m_Q . One sees that the state is almost purely in the λ mode at $m_Q \geq 1.5$ GeV; the λ dominance is seen even at $m_Q = 510$ MeV. As is classified in TABLE VI, the quark model predicts seven P -wave Λ_Q excitations, $(1/2^-)^3$, $(3/2^-)^3$, $(5/2^-)$. They split into the $(1/2^-, 3/2^-)$ λ modes and $(1/2^-)^2$, $(3/2^-)^2$, $5/2^-$ ρ modes. In Fig. 9, one sees clear splitting (≈ 350 MeV) of two low lying λ -modes and five higher ρ mode states.

The P -wave Σ_Q has also seven states in the quark model, $(1/2^-)^3$, $(3/2^-)^3$, $(5/2^-)$. One sees that they are classified into the $(1/2)^2$, $(3/2^-)^2$, $(5/2^-)$ λ modes and $(1/2^-, 3/2^-)$ ρ modes from Fig.9. The λ - and ρ - modes are separated more slowly than Λ_Q as m_Q increases, and the λ dominance is seen at $m_Q \geq 1750$ MeV. The difference comes from the interaction between light quarks which forms the diquark. The diquark in Σ_Q has spin 1 and the spin-spin interaction is repulsive for the λ mode, while the ρ mode has a diquark state of spin 0 and the

(a) Λ_c			(b) Σ_c			(c) Ω_c		
J^P	Theory [MeV]	Exp. [MeV]	J^P	Theory [MeV]	Exp. [MeV]	J^P	Theory [MeV]	Exp. [MeV]
$\frac{1}{2}^+$	2285	2285	$\frac{1}{2}^+$	2460	2455	$\frac{1}{2}^+$	2731	2698
	2857			3029			3227	
	3123			3103			3292	
$\frac{3}{2}^+$	2920		$\frac{3}{2}^+$	2523	2518	$\frac{3}{2}^+$	2779	2768
	3175			3065			3257	
	3191			3094			3285	
$\frac{5}{2}^+$	2922	2881	$\frac{5}{2}^+$	3099		$\frac{5}{2}^+$	3288	
	3202			3114			3299	
	3230			3191			3359	
$\frac{1}{2}^-$	2628	2595	$\frac{1}{2}^-$	2802		$\frac{1}{2}^-$	3030	
	2890			2826			3048	
	2933			2909			3110	
$\frac{3}{2}^-$	2630	2628	$\frac{3}{2}^-$	2807		$\frac{3}{2}^-$	3033	
	2917			2837			3056	
	2956			2910			3111	
$\frac{5}{2}^-$	2960		$\frac{5}{2}^-$	2839		$\frac{5}{2}^-$	3057	
	3444			3316			3477	
	3491			3521			3620	

TABLE VII: Calculated energy spectra and experimental result of Λ_c , Σ_c , Ω_c

spin-spin interaction is attractive. Therefore, the difference between the excitation energies of the two modes is small compared to Λ_Q . Thus, the splitting between the excitation energies of two modes is larger for Λ_Q and smaller for Σ_Q compared with the case in which there is no spin-spin force as we see in Sec.I. As a result, the change of the probability of two modes in the Σ_Q case is more slow than the Λ_Q case as shown in Fig.11.

D. Heavy baryons in the heavy quark limit

In this subsection, we investigate the behavior of the single-heavy baryons in the heavy quark limit. We decompose the wave functions of the P-wave single-heavy baryons into the parts with different light spin component j as

$$\begin{aligned} \Phi_{\Lambda_Q}^{J=1/2,M}(\boldsymbol{\rho}, \boldsymbol{\lambda}) &= \phi_{\Lambda_Q, j=0}^{J=1/2,M}(\boldsymbol{\rho}, \boldsymbol{\lambda}) \\ &+ \phi_{\Lambda_Q, j=1}^{J=1/2,M}(\boldsymbol{\rho}, \boldsymbol{\lambda}) \end{aligned} \quad (42)$$

$$\begin{aligned} \Phi_{\Lambda_Q}^{J=3/2,M}(\boldsymbol{\rho}, \boldsymbol{\lambda}) &= \phi_{\Lambda_Q, j=1}^{J=3/2,M}(\boldsymbol{\rho}, \boldsymbol{\lambda}) \\ &+ \phi_{\Lambda_Q, j=2}^{J=3/2,M}(\boldsymbol{\rho}, \boldsymbol{\lambda}) \end{aligned} \quad (43)$$

$$\begin{aligned} \Phi_{\Sigma_Q}^{J=1/2,M}(\boldsymbol{\rho}, \boldsymbol{\lambda}) &= \phi_{\Sigma_Q, j=0}^{J=1/2,M}(\boldsymbol{\rho}, \boldsymbol{\lambda}) \\ &+ \phi_{\Sigma_Q, j=1}^{J=1/2,M}(\boldsymbol{\rho}, \boldsymbol{\lambda}) \end{aligned} \quad (44)$$

$$\begin{aligned} \Phi_{\Sigma_Q}^{J=3/2,M}(\boldsymbol{\rho}, \boldsymbol{\lambda}) &= \phi_{\Sigma_Q, j=1}^{J=3/2,M}(\boldsymbol{\rho}, \boldsymbol{\lambda}) \\ &+ \phi_{\Sigma_Q, j=2}^{J=3/2,M}(\boldsymbol{\rho}, \boldsymbol{\lambda}). \end{aligned} \quad (45)$$

In the case of double-heavy baryon, the λ -mode state is composed of the $(QQ)_{\ell=0}$ heavy diquark with the light quark q , while the ρ -mode state has the excited heavy diquark $(QQ)_{\ell=1}$ in the $L=0$ orbit around q . The combinations of angular momentum are the same as the Σ_Q case which is shown in TABLE VI, but the behavior of λ - and ρ modes are different because Ξ_{QQ} , or Ω_{QQ} contains heavy diquark. As mentioned in Sec.I, ω_λ is larger than ω_ρ for the P wave double-heavy baryons and thus ρ modes are dominant. This is shown in Fig.10 and Fig.12. One sees that the $(1/2)^2$, $(3/2^-)^2$, $(5/2^-)$ λ modes and the $(1/2^-, 3/2^-)$ ρ modes split in the heavy quark region in Fig.10, and the ρ modes become dominant for the lowest states at $m_Q \geq m_c$ in Fig.12.

(a) Λ_b			(b) Σ_b			(c) Ω_b		
J^P	Theory [MeV]	Exp. [MeV]	J^P	Theory [MeV]	Exp. [MeV]	J^P	Theory [MeV]	Exp. [MeV]
$\frac{1}{2}^+$	5618	5624	$\frac{1}{2}^+$	5823	5815	$\frac{1}{2}^+$	6076	6048
	6153			6343			6517	
	6467			6395			6561	
$\frac{3}{2}^+$	6211		$\frac{3}{2}^+$	5845	5835	$\frac{3}{2}^+$	6094	
	6488			6356			6528	
	6511			6393			6559	
$\frac{5}{2}^+$	6212		$\frac{5}{2}^+$	6397		$\frac{5}{2}^+$	6561	
	6530			6402			6566	
	6539			6505			6657	
$\frac{1}{2}^-$	5938	5912	$\frac{1}{2}^-$	6127		$\frac{1}{2}^-$	6333	
	6236			6135			6340	
	6273			6246			6437	
$\frac{3}{2}^-$	5939	5920	$\frac{3}{2}^-$	6132		$\frac{3}{2}^-$	6336	
	6273			6141			6344	
	6285			6246			6438	
$\frac{5}{2}^-$	6289		$\frac{5}{2}^-$	6144		$\frac{5}{2}^-$	6345	
	6739			6592			6728	
	6786			6834			6919	

TABLE VIII: Calculated energy spectra and experimental result of Λ_b , Σ_b , Ω_b

Here, we take into account only the channel $c = 3$ of the Jacobi coordinates, given in Fig.2. The relation between the representation Eq.(42)-(45) and Eq.(15) is shown in Appendix A. The heavy quark mass dependences of the probabilities of each j state are shown in the Figs.13-16 (See Appendix A for the definition). The mixings between $j = 0$ and $j = 1$ or $j = 1$ and $j = 2$ above 1 GeV are negligible for the first state of $\Lambda_Q(1/2^-)$ and $\Lambda_Q(3/2^-)$ and the third state of $\Sigma_Q(1/2^-)$ and $\Sigma_Q(3/2^-)$, which correspond to red lines in Figs 13-14 and green lines in Figs.15-16. This is because these states are isolated from the other states, as is shown in Fig.9. For the other state, two different j components (five λ -modes of Σ_Q and five ρ -modes of Λ_Q) still mix in the charm and bottom mass region, because they lie close to each other within 50 MeV (See Fig.9). Above $m_Q = 14$ GeV, one sees no mixing between different j components. In summary, one finds that the second $1/2^-$ state of Λ_Q and the first $1/2^-$ state of $1/2^-$ of Σ_Q are the $j=0$ singlet state. All the other belong to doublets, $(1/2_1^-, 3/2_1^-)$, $(1/2_3^-, 3/2_2^-)$ and $(3/2_3^-, 5/2_1^-)$ for Λ_Q and $(1/2_2^-, 3/2_1^-)$, $(3/2_2^-, 5/2_1^-)$ and $(1/2_3^-, 3/2_2^-)$ for Σ_Q , as is shown in Fig.9.

We next discuss the positive parity states. We focus on the first six positive parity state of single-heavy baryons, corresponding to the states below 3.0 GeV in the charm sector (See Fig.5). They consist of the S-wave

$((L, \ell) = (0, 0))$ component, the $(1, 1)$ component, the $(2, 0)$ component (ρ -mode) and the $(0, 2)$ component (λ -mode). Figs.17-22 show the probabilities of the each component in the total wave function. One sees that one component becomes dominant above $m_Q = 1$ GeV. The $(0, 0)$ component is dominant for $\Lambda_Q(1/2_1^+)$, $\Lambda_Q(1/2_2^+)$, $\Sigma_Q(1/2_1^+)$, $\Sigma_Q(1/2_2^+)$ and $(2, 0)$ component (λ -mode) is dominant for $\Lambda_Q(3/2_1^+)$, $\Lambda_Q(5/2_1^+)$ above 1 GeV (See Figs.17-22). The lowest six states in the heavy quark region can be written as follows.

$$\Phi_{\Lambda_Q}^{J_n=1/2_1, M}(\boldsymbol{\rho}, \boldsymbol{\lambda}) = \phi_{\Lambda_Q, j=0}^{J_n=1/2_1^+, M}(\boldsymbol{\rho}, \boldsymbol{\lambda}) \quad (46)$$

$$\Phi_{\Lambda_Q}^{J_n=1/2_2, M}(\boldsymbol{\rho}, \boldsymbol{\lambda}) = \phi_{\Lambda_Q, j=0}^{J_n=1/2_2^+, M}(\boldsymbol{\rho}, \boldsymbol{\lambda}) \quad (47)$$

$$\Phi_{\Lambda_Q}^{J_n=3/2_1, M}(\boldsymbol{\rho}, \boldsymbol{\lambda}) = \phi_{\Lambda_Q, j=2}^{J_n=3/2_1^+, M}(\boldsymbol{\rho}, \boldsymbol{\lambda}) \quad (48)$$

$$\Phi_{\Lambda_Q}^{J_n=5/2_1, M}(\boldsymbol{\rho}, \boldsymbol{\lambda}) = \phi_{\Lambda_Q, j=2}^{J_n=5/2_1^+, M}(\boldsymbol{\rho}, \boldsymbol{\lambda}) \quad (49)$$

$$\Phi_{\Sigma_Q}^{J_n=1/2_1, M}(\boldsymbol{\rho}, \boldsymbol{\lambda}) = \phi_{\Sigma_Q, j=1}^{J_n=1/2_1^+, M}(\boldsymbol{\rho}, \boldsymbol{\lambda}) \quad (50)$$

(a) Ξ_{cc}					(b) Ξ_{bb}			
J^P	Theory [MeV]	Exp. [MeV]	[14]	[9]	J^P	Theory [MeV]	[9] [MeV]	
$\frac{1}{2}^+$	3685	3512	3603±15±16	3674	$\frac{1}{2}^+$	10314	10340	
	4079			4029		10571		
	4159					10612		
$\frac{3}{2}^+$	3754		3706±22±16	3753	$\frac{3}{2}^+$	10339	10367	
	4114			4042		10592		
	4131					10593		
$\frac{5}{2}^+$	4115			4047	$\frac{5}{2}^+$	10592	10676	
	4164			4091		10613		
	4348					10809		
$\frac{1}{2}^-$	3947			3910	$\frac{1}{2}^-$	10476	10493	
	4135			4074		10703		
	4149					10740		
$\frac{3}{2}^-$	3949			3921	$\frac{3}{2}^-$	10476	10495	
	4137			4078		10704		
	4159					10742		
$\frac{5}{2}^-$	4163			4092	$\frac{5}{2}^-$	10759	10713	
	4488					10973		
	4534					11004		

TABLE IX: Calculated energy spectra and experimental result of Ξ_{cc} and Ξ_{bb}

$$\Phi_{\Sigma_Q}^{J_n=3/2_1, M}(\rho, \lambda) = \phi_{\Sigma_Q, j=1}^{J_n=3/2_1, M}(\rho, \lambda) \quad (51)$$

where we use Eq.(41) to transform the bases. There are two doublet pairs ($\Lambda_Q(3/2_1^+)$, $\Lambda_Q(5/2_1^+)$) ($j = 2$), ($\Sigma_Q(1/2_1^+)$, $\Sigma_Q(3/2_1^+)$) ($j = 1$) and two singlet states $\Lambda_Q(1/2_1^+)$, $\Lambda_Q(1/2_2^+)$ in the heavy quark limit. Mixings of different j components of the wave function are negligible even in the charm quark region.

IV. SUMMARY

We have studied the spectrum of the single- and double-heavy baryons and discussed their structures within the framework of a constituent quark model. The potential parameters are determined so as to reproduce the energies of the lowest states $\Lambda(1/2^+)$, $\Sigma(1/2^+)$, $\Sigma(3/2^+)$, $\Lambda(1/2^-)$, $\Lambda(3/2^-)$, $\Lambda_c(1/2^+)$ and $\Lambda_b(1/2^+)$. In the analysis of the baryon wave functions, we have focused on the two characteristic excited modes and investigated their probabilities as functions of the heavy quark mass. To obtain the precise energy eigenvalues of excited states, we employ the gaussian expansion method, which is one of the best methods for three and four body bound states. We have obtained the followings:

(1) Masses of the known Λ_Q , Σ_Q and Ω_Q are in good

agreement with the observed data within 50 MeV. Then, we predicted that observed $\Sigma_c(2800)$ can be assigned to $1/2_1^-$, $3/2_1^-$, $1/2_2^-$, $3/2_2^-$ and $5/2_1^-$ state, and Λ_c to $3/2_1^+$, $5/2_1^+$, $1/2_2^+$, $1/2_3^+$ and $3/2_2^-$ and $3/2_3^-$.

(2) In the heavy quark limit, we find six doublets and two singlets for the P-wave single-heavy baryons (See Fig.9) and two doublets and two singlets for the first six states of positive parity single-heavy baryons. In the charm sector, the mass differences of these heavy quark spin-doublets are less than 30 [MeV] and in the bottom sector, the differences reduce to less than 10 [MeV].

(3) For the double-heavy baryons, we predict that the mass of the ground Ξ_{cc} state is $\Xi_{cc}(3685)$. This result is consistent with the recent Lattice QCD calculations within 50 MeV. Experimentally, it was reported that a double-charmed baryon was found at the mass 3512 MeV [17]. But other experimental groups, LHC and Belle, have not yet succeeded in observing the state.

(4) We have investigated the dependences on the heavy quark mass m_Q of the λ and ρ modes to see the features of the negative parity states. Mixings of the ρ and λ modes are suppressed and only one mode dominates. This is because the spin-spin interaction which mainly causes the mixing becomes small in the heavy quark region. It is a

(a) Ω_{cc}				(b) Ω_{bb}			
J^P	Theory [MeV]	[14]	[9]	J^P	Theory [MeV]	[9]	
$\frac{1}{2}^+$	3832	3704±5±16	3815	$\frac{1}{2}^+$	10447	10454	
	4227		4180		10707	10693	
	4295				10744		
$\frac{3}{2}^+$	3883	3779±6±17	3876	$\frac{3}{2}^+$	10467	10486	
	4263		4188		10723	10721	
	4265				10730		
$\frac{5}{2}^+$	4264		4202	$\frac{5}{2}^+$	10729	10720	
	4299		4232		10744	10734	
	4410				10937		
$\frac{1}{2}^-$	4086		4046	$\frac{1}{2}^-$	10607	10616	
	4199		4135		10796	10763	
	4210				10803		
$\frac{3}{2}^-$	4086		4052	$\frac{3}{2}^-$	10608	10619	
	4201		4140		10797	10765	
	4218				10805		
$\frac{5}{2}^-$	4220		4152	$\frac{5}{2}^-$	10808	10766	
	4555				11028		
	4600				11059		

TABLE X: Calculated energy spectra and experimental result of Ω_{cc} and Ω_{bb}

future problem to clarify what physical quantities sensitive the differences of the two modes. One possibility is decay patterns. It is conjectured that the λ -mode states decay dominantly to a light baryon and a heavy meson, while the ρ -mode states decay mostly into a light meson and a heavy baryon. Further studies of the decays and productions of these heavy baryons will be useful to verify more on these structures.

Acknowledgments

The authors would like to thank Drs. Shigehiro Yasui, Hiroyuki Noumi for valuable discussions. This work was supported in part by JSPS KAKENHI numbers, 25247036, 24250294, 26400273. T.Y. acknowledges the Junior Research Associate scholarship at RIKEN. The numerical calculations were carried out on SR16000 at YITP in Kyoto University.

Appendix A: The transformation of the bases

We discuss the wave function in the heavy quark limit in this appendix. For the single-heavy baryons, we take only the channel $c=3$ of the Jacobi coordinate given in Fig.2. The P-wave wave functions of the Λ_Q and Σ_Q

baryons are given by the sum of the λ -mode ($^{2S+1}\lambda = ^2\lambda, ^4\lambda$) and ρ -mode ($^{2S+1}\rho = ^2\rho, ^4\rho$) components as follows.

$$\begin{aligned}
\Phi_{\Lambda_Q}^{JM}(\boldsymbol{\rho}, \boldsymbol{\lambda}) &= \psi_{2\rho}^{\Lambda_Q} \sum_{(n,N)} C_{n,N}^{2\rho} \phi_{n,N}(\boldsymbol{\rho}, \boldsymbol{\lambda}) \\
&+ \psi_{4\rho}^{\Lambda_Q} \sum_{(n,N)} C_{n,N}^{4\rho} \phi_{n,N}(\boldsymbol{\rho}, \boldsymbol{\lambda}) \\
&+ \psi_{2\lambda}^{\Lambda_Q} \sum_{(n,N)} C_{n,N}^{2\lambda} \phi_n(\boldsymbol{\rho}, \boldsymbol{\lambda}) \quad (A1)
\end{aligned}$$

$$\begin{aligned}
\Phi_{\Sigma_Q}^{JM}(\boldsymbol{\rho}, \boldsymbol{\lambda}) &= \psi_{2\lambda}^{\Sigma_Q} \sum_{(n,N)} C_{n,N}^{2\lambda} \phi_n(\boldsymbol{\rho}, \boldsymbol{\lambda}) \\
&+ \psi_{4\lambda}^{\Sigma_Q} \sum_{(n,N)} C_n^{4\lambda} \phi_{n,N}(\boldsymbol{\rho}, \boldsymbol{\lambda}) \\
&+ \psi_{2\rho}^{\Sigma_Q} \sum_{(n,N)} C_{n,N}^{2\rho} \phi_{n,N}(\boldsymbol{\rho}, \boldsymbol{\lambda}). \quad (A2)
\end{aligned}$$

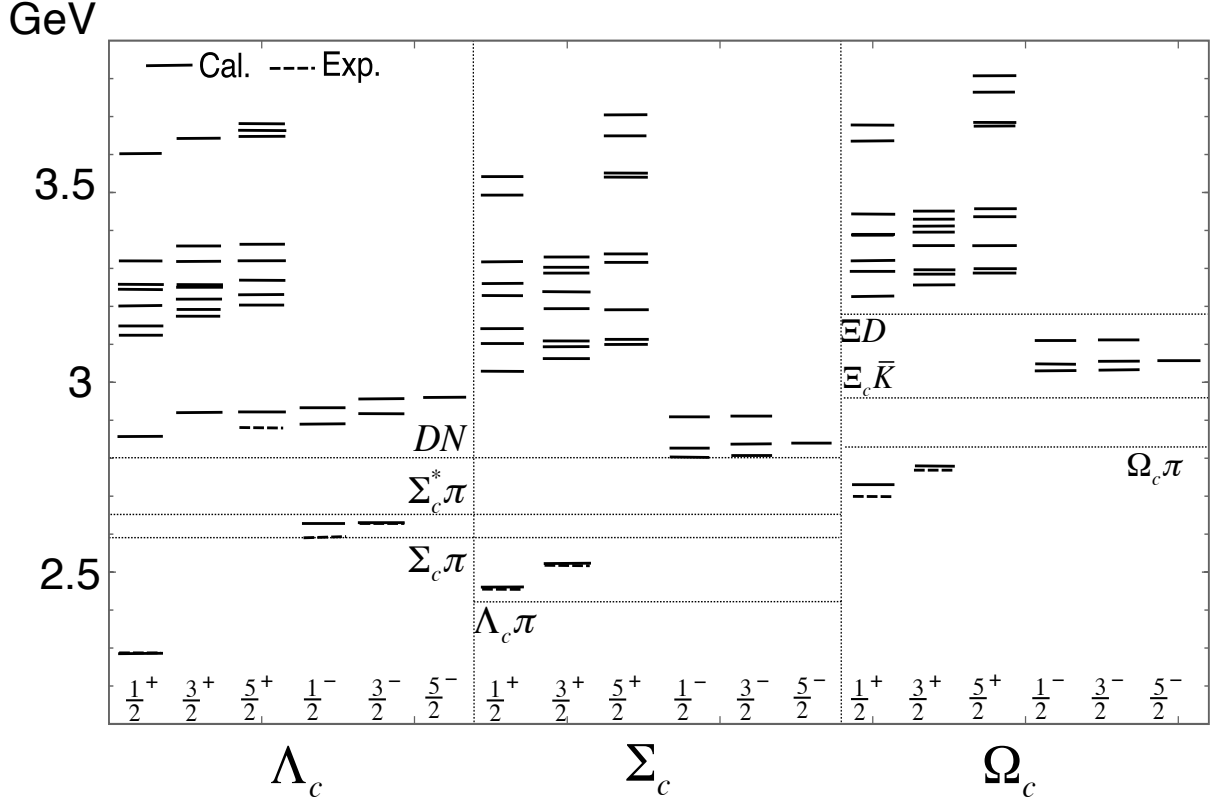


FIG. 5: Calculated energy spectra of Λ_c , Σ_c , Ω_c for $1/2^+$, $3/2^+$, $5/2^+$, $1/2^-$, $3/2^-$, $5/2^-$ (solid line) together with experimental data (dashed line). Several thresholds are also shown by dotted line.

Here we extract the parts of the spin and orbital angular momenta for each mode as

$$\psi_{2\rho}^{\Lambda_Q} = [X_{S=1/2,1}[Y_{\ell=1}(\hat{\rho})Y_{L=0}(\hat{\lambda})]_{I=1}]_{JM} \quad (\text{A3})$$

$$\psi_{4\rho}^{\Lambda_Q} = [X_{S=3/2,1}[Y_{\ell=1}(\hat{\rho})Y_{L=0}(\hat{\lambda})]_{I=1}]_{JM} \quad (\text{A4})$$

$$\psi_{2\lambda}^{\Lambda_Q} = [X_{S=1/2,0}[Y_{\ell=0}(\hat{\rho})Y_{L=1}(\hat{\lambda})]_{I=1}]_{JM} \quad (\text{A5})$$

$$\psi_{2\lambda}^{\Sigma_Q} = [X_{S=1/2,1}[Y_{\ell=0}(\hat{\rho})Y_{L=1}(\hat{\lambda})]_{I=1}]_{JM} \quad (\text{A6})$$

$$\psi_{4\lambda}^{\Sigma_Q} = [X_{S=3/2,1}[Y_{\ell=0}(\hat{\rho})Y_{L=1}(\hat{\lambda})]_{I=1}]_{JM} \quad (\text{A7})$$

$$\psi_{2\rho}^{\Sigma_Q} = [X_{S=1/2,0}[Y_{\ell=1}(\hat{\rho})Y_{L=0}(\hat{\lambda})]_{I=1}]_{JM} \quad (\text{A8})$$

Then the corresponding radial parts are expanded by the Gaussian basis as

$$\phi_{n,N}(\rho, \lambda) = N_{n\ell} N_{NL} \rho^\ell e^{-\beta_n \rho^2} \lambda^L e^{-\gamma_N \lambda^2}, \quad (\text{A9})$$

where $N_{n\ell}$ (N_{NL}) is the normalization constant. As is discussed in Sec.III.C, the light spin component j is con-

served in the heavy quark limit. Therefore, we transform the bases into those which diagonalize j . We use Eq.(41) to transform the bases, and obtain

$$\psi_{2\rho}^{\Lambda_Q} = \sqrt{\frac{1}{3}}\psi_{j=0,s=1} - \sqrt{\frac{2}{3}}\psi_{j=1,s=1} \quad (\text{A10})$$

$$\psi_{4\rho}^{\Lambda_Q} = \sqrt{\frac{2}{3}}\psi_{j=0,s=1} + \sqrt{\frac{1}{3}}\psi_{j=1,s=1} \quad (\text{A11})$$

$$\psi_{2\lambda}^{\Lambda_Q} = -\psi_{j=1,s=0} \quad (\text{A12})$$

$$\psi_{2\lambda}^{\Sigma_Q} = \sqrt{\frac{1}{3}}\psi_{j=0,s=1} - \sqrt{\frac{2}{3}}\psi_{j=1,s=1} \quad (\text{A13})$$

$$\psi_{4\lambda}^{\Sigma_Q} = \sqrt{\frac{2}{3}}\psi_{j=0,s=1} + \sqrt{\frac{1}{3}}\psi_{j=1,s=1} \quad (\text{A14})$$

$$\psi_{2\rho}^{\Sigma_Q} = -\psi_{j=1,s=0}. \quad (\text{A15})$$

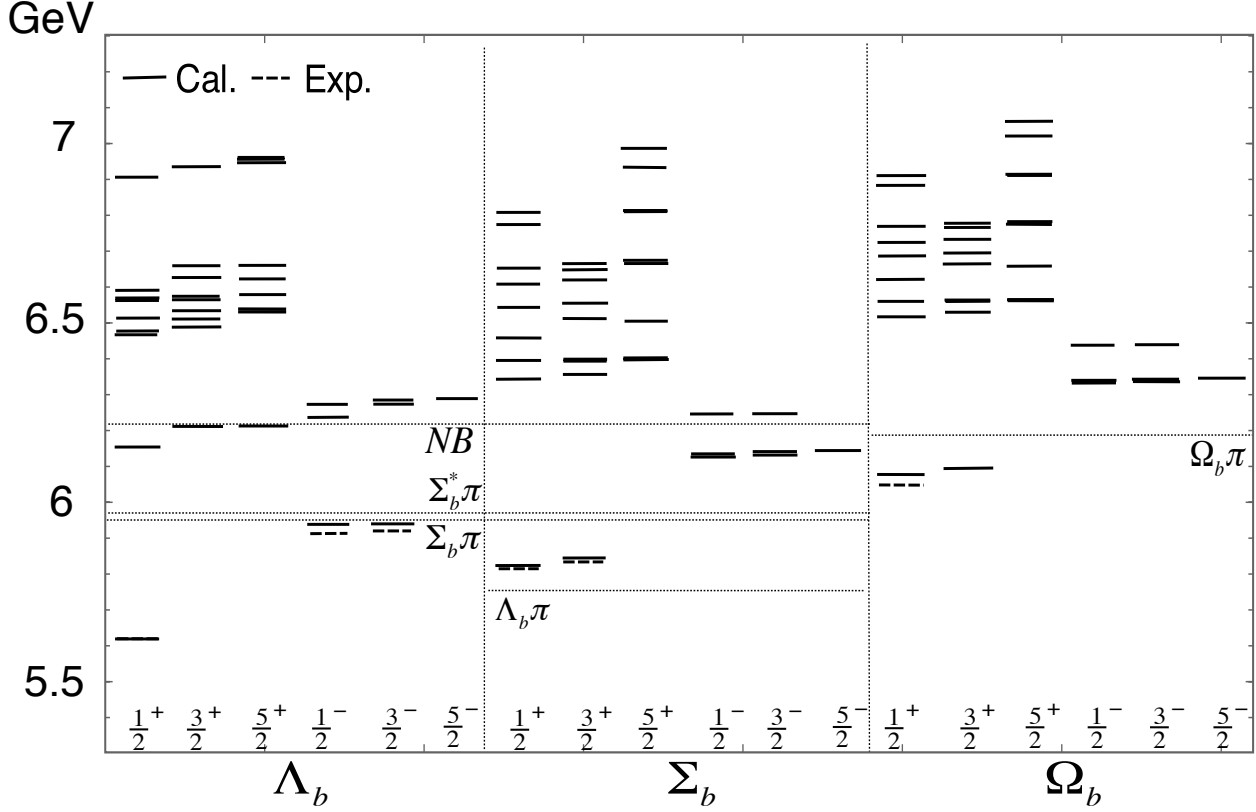


FIG. 6: Calculated energy spectra of Λ_b , Σ_b , Ω_b for $1/2^+$, $3/2^+$, $5/2^+$, $1/2^-$, $3/2^-$, $5/2^-$ (solid line) together with experimental data(dashed line).Several thresholds are also shown by dotted line.

for $J = 1/2^-$ and

$$\psi_{2\rho}^{\Lambda_Q} = -\sqrt{\frac{1}{6}}\psi_{j=1,s=1} + \sqrt{\frac{5}{6}}\psi_{j=2,s=1} \quad (\text{A16})$$

$$\psi_{4\rho}^{\Lambda_Q} = -\sqrt{\frac{5}{6}}\psi_{j=1,s=1} - \sqrt{\frac{1}{6}}\psi_{j=2,s=1} \quad (\text{A17})$$

$$\psi_{2\lambda}^{\Lambda_Q} = \psi_{j=1,s=0} \quad (\text{A18})$$

$$\psi_{2\lambda}^{\Sigma_Q} = -\sqrt{\frac{1}{6}}\psi_{j=1,s=1} + \sqrt{\frac{5}{6}}\psi_{j=2,s=1} \quad (\text{A19})$$

$$\psi_{4\lambda}^{\Sigma_Q} = -\sqrt{\frac{5}{6}}\psi_{j=1,s=1} - \sqrt{\frac{1}{6}}\psi_{j=2,s=1} \quad (\text{A20})$$

$$\psi_{2\rho}^{\Sigma_Q} = \psi_{j=1,s=0}. \quad (\text{A21})$$

for $J = 3/2^-$, where

$$\psi_{j,s} = [[[\chi_{1/2}(q)\chi_{1/2}(q)]_s[Y(\hat{\rho})_\ell Y(\hat{\lambda})_L]_l]_j\chi_{1/2}(Q)]_J \quad (\text{A22})$$

By using Eq.(A3)-(A8), Eq.(A1) and Eq(A2) is transformed into the bases which is characterized by j .

• $\Lambda_Q(1/2^-, 3/2^-)$

$$\begin{aligned} \phi_{\Lambda_Q,j=0}^{J=1/2,M}(\rho, \lambda) &= \psi_{j=0,s=1} \left(\sqrt{\frac{1}{3}} \sum_{(n,N)} C_{n,N}^{2\rho} \phi_{n,N}(\rho, \lambda) \right. \\ &\quad \left. + \sqrt{\frac{2}{3}} \sum_{(n,N)} C_{n,N}^{4\rho} \phi_{n,N}(\rho, \lambda) \right) \\ &\quad - \psi_{j=0,s=0} \sum_{(n,N)} C_{n,N}^{2\lambda} \phi_{n,N}(\rho, \lambda) \quad (\text{A23}) \end{aligned}$$

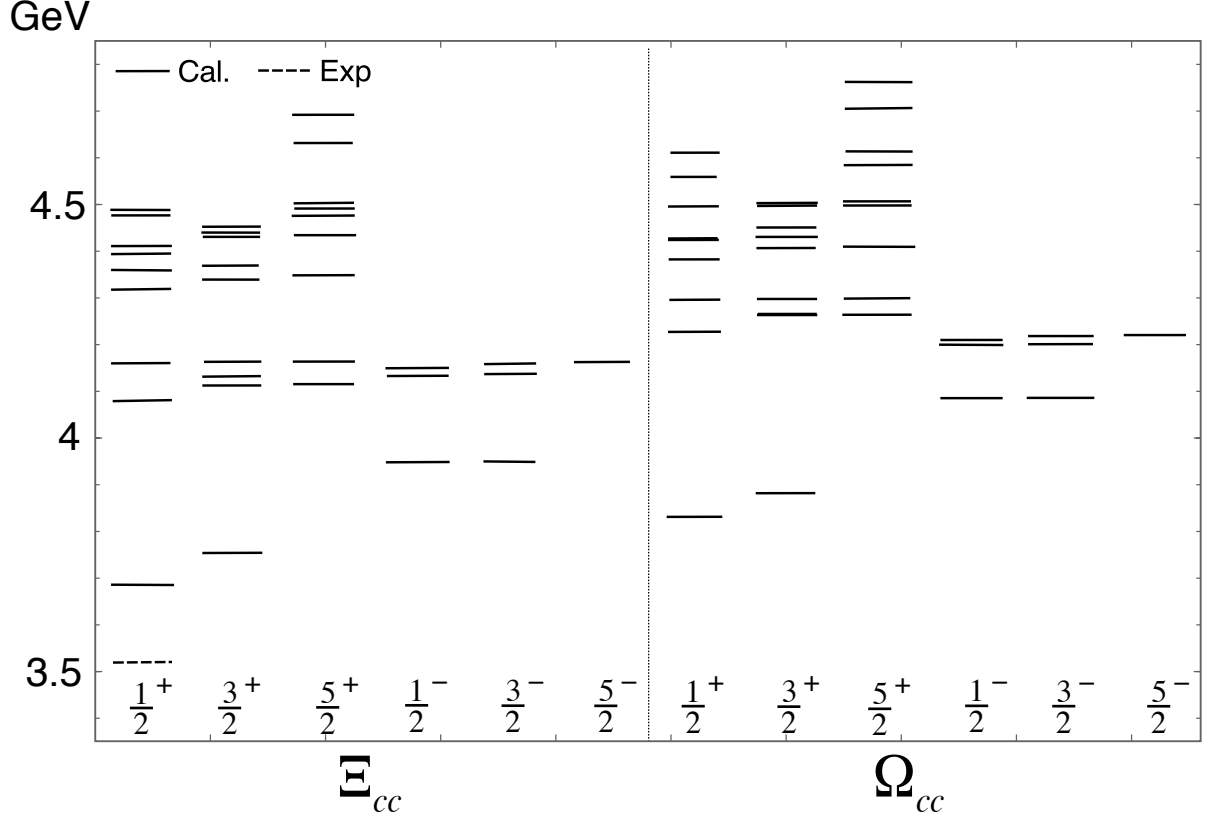


FIG. 7: Calculated energy spectra of Ξ_{cc} , Ω_{cc} for $1/2^+$, $3/2^+$, $5/2^+$, $1/2^-$, $3/2^-$, $5/2^-$ (solid line) together with experimental data (dashed line).

$$\begin{aligned} \phi_{\Lambda_Q, j=1}^{J=1/2, M}(\rho, \lambda) &= \psi_{j=1, s=1} \left(-\sqrt{\frac{2}{3}} \sum_{(n, N)} C_{n, N}^{2\rho} \phi_{n, N}(\rho, \lambda) \right. \\ &\quad \left. + \sqrt{\frac{1}{3}} \sum_{(n, N)} C_{n, N}^{4\rho} \phi_{n, N}(\rho, \lambda) \right) \quad (\text{A24}) \end{aligned}$$

$$\begin{aligned} \phi_{\Lambda_Q, j=1}^{J=3/2, M}(\rho, \lambda) &= \psi_{j=1, s=1} \left(-\sqrt{\frac{1}{6}} \sum_{(n, N)} C_{n, N}^{2\rho} \phi_{n, N}(\rho, \lambda) \right. \\ &\quad \left. - \sqrt{\frac{5}{6}} \sum_{(n, N)} C_{n, N}^{4\rho} \phi_{n, N}(\rho, \lambda) \right) \\ &\quad + \psi_{j=1, s=0} \sum_{(n, N)} C_{n, N}^{2\lambda} \phi_{n, N}(\rho, \lambda) \quad (\text{A25}) \end{aligned}$$

$$\begin{aligned} \phi_{\Lambda_Q, j=2}^{J=3/2, M}(\rho, \lambda) &= \psi_{j=2, s=1} \left(\sqrt{\frac{5}{6}} \sum_{(n, N)} C_{n, N}^{2\rho} \phi_{n, N}(\rho, \lambda) \right. \\ &\quad \left. - \sqrt{\frac{1}{6}} \sum_{(n, N)} C_{n, N}^{4\rho} \phi_{n, N}(\rho, \lambda) \right) \quad (\text{A26}) \end{aligned}$$

• $\Sigma_Q(1/2^-, 3/2^-)$

$$\begin{aligned} \phi_{\Sigma_Q, j=0}^{J=1/2, M}(\rho, \lambda) &= \psi_{j=0, s=1} \left(\sqrt{\frac{1}{3}} \sum_{(n, N)} C_{n, N}^{2\lambda} \phi_{n, N}(\rho, \lambda) \right. \\ &\quad \left. + \sqrt{\frac{2}{3}} \sum_{(n, N)} C_{n, N}^{4\lambda} \phi_{n, N}(\rho, \lambda) \right) \\ &\quad - \psi_{j=0, s=0} \sum_{(n, N)} C_{n, N}^{2\rho} \phi_{n, N}(\rho, \lambda) \quad (\text{A27}) \end{aligned}$$

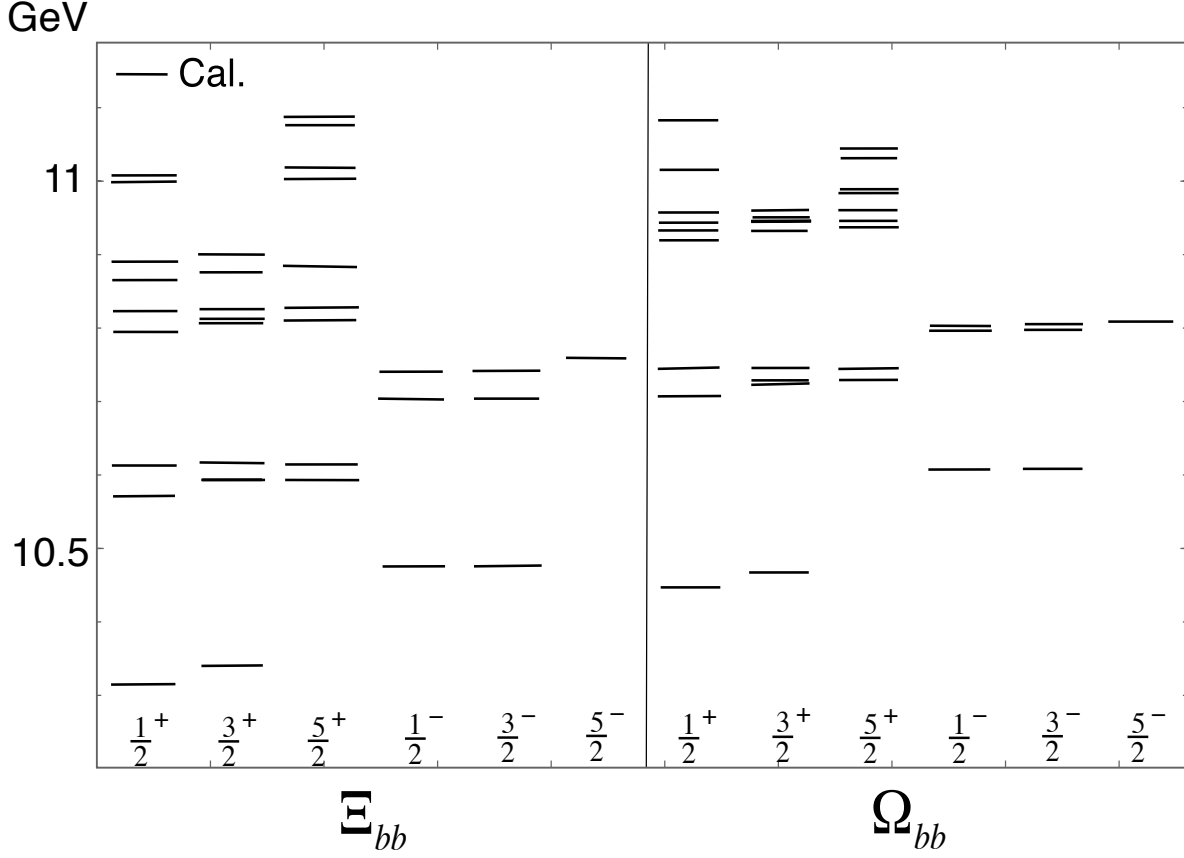


FIG. 8: Calculated energy spectra of Ξ_{bb} , Ω_{bb} for $1/2^+$, $3/2^+$, $5/2^+$, $1/2^-$, $3/2^-$, $5/2^-$ (solid line) together with experimental data (dashed line).

$$\begin{aligned} \phi_{\Sigma_Q, j=1}^{J=1/2, M}(\boldsymbol{\rho}, \boldsymbol{\lambda}) = & \psi_{j=1, s=1} \left(-\sqrt{\frac{2}{3}} \sum_{(n, N)} C_{n, N}^{2\lambda} \phi_{n, N}(\rho, \lambda) \right. \\ & \left. + \sqrt{\frac{1}{3}} \sum_{(n, N)} C_{n, N}^{4\lambda} \phi_{n, N}(\rho, \lambda) \right) \quad (\text{A28}) \end{aligned}$$

$$\begin{aligned} \phi_{\Sigma_Q, j=2}^{J=3/2, M}(\boldsymbol{\rho}, \boldsymbol{\lambda}) = & \psi_{j=2, s=1} \left(\sqrt{\frac{5}{6}} \sum_{(n, N)} C_{n, N}^{2\lambda} \phi_{n, N}(\rho, \lambda) \right. \\ & \left. - \sqrt{\frac{1}{6}} \sum_{(n, N)} C_{n, N}^{4\lambda} \phi_{n, N}(\rho, \lambda) \right) \quad (\text{A30}) \end{aligned}$$

$$\begin{aligned} \phi_{\Sigma_Q, j=1}^{J=3/2, M}(\boldsymbol{\rho}, \boldsymbol{\lambda}) = & \psi_{j=1, s=1} \left(-\sqrt{\frac{1}{6}} \sum_{(n, N)} C_{n, N}^{2\lambda} \phi_{n, N}(\rho, \lambda) \right. \\ & \left. - \sqrt{\frac{5}{6}} \sum_{(n, N)} C_{n, N}^{4\lambda} \phi_{n, N}(\rho, \lambda) \right) \\ & + \psi_{j=1, s=0} \sum_{(n, N)} C_{n, N}^{2\rho} \phi_{n, N}(\rho, \lambda) \quad (\text{A29}) \end{aligned}$$

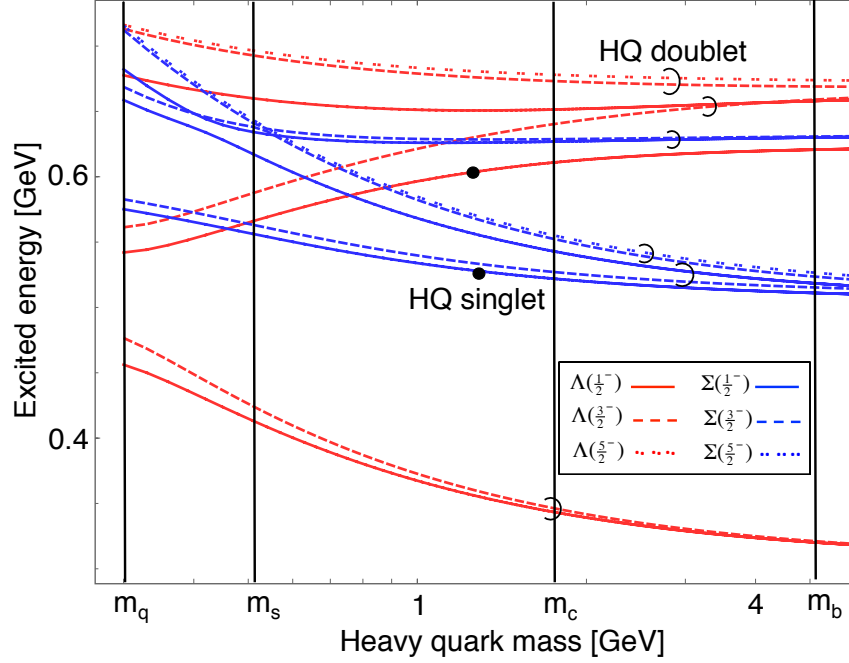


FIG. 9: Heavy quark mass dependence of excited energy of first state, second state and third state for $1/2^-$ (solid line), $3/2^-$ (dashed line), $5/2^-$ (twined line) of Λ_Q (red line) and Σ_Q (blue line). Bullet denote heavy quark singlet. The pair within a half circle denote heavy quark doublet.

-
- [1] M. Voloshin, *Prog.Part.Nucl.Phys.* **61**, 455 (2008), [arXiv:0711.4556 \[hep-ph\]](#).
- [2] S. Ohkoda, Y. Yamaguchi, S. Yasui, K. Sudoh, and A. Hosaka, *Phys.Rev.* **D86**, 014004 (2012), [arXiv:1111.2921 \[hep-ph\]](#).
- [3] R. Aaij *et al.* (LHCb), *Phys. Rev. Lett.* **115**, 072001 (2015), [arXiv:1507.03414 \[hep-ex\]](#).
- [4] S. H. Lee, S. Yasui, W. Liu, and C. M. Ko, *Eur.Phys.J.* **C54**, 259 (2008), [arXiv:0707.1747 \[hep-ph\]](#).
- [5] L. Maiani, F. Piccinini, A. Polosa, and V. Riquer, *Phys.Rev.* **D71**, 014028 (2005), [arXiv:hep-ph/0412098 \[hep-ph\]](#).
- [6] A. Selem and F. Wilczek, *New trends in HERA physics. Proceedings, Ringberg Workshop, Tegernsee, Germany, October 2-7, 2005* (2006), [arXiv:hep-ph/0602128 \[hep-ph\]](#).
- [7] C. Alexandrou, P. de Forcrand, and B. Lucini, *Phys.Rev.Lett.* **97**, 222002 (2006), [arXiv:hep-lat/0609004 \[hep-lat\]](#).
- [8] L. Copley, N. Isgur, and G. Karl, *Phys.Rev.* **D20**, 768 (1979).
- [9] W. Roberts and M. Pervin, *Int.J.Mod.Phys.* **A23**, 2817 (2008), [arXiv:0711.2492 \[nucl-th\]](#).
- [10] Y. Yamaguchi, S. Ohkoda, A. Hosaka, T. Hyodo, and S. Yasui, *Phys. Rev.* **D91**, 034034 (2015), [arXiv:1402.5222 \[hep-ph\]](#).
- [11] T. Kawanai and S. Sasaki, *Phys.Rev.Lett.* **107**, 091601 (2011), [arXiv:1102.3246 \[hep-lat\]](#).
- [12] S. Takeuchi, *Phys.Rev.Lett.* **73**, 2173 (1994).
- [13] E. Hiyama, Y. Kino, and M. Kamimura, *Prog.Part.Nucl.Phys.* **51**, 223 (2003).
- [14] Y. Namekawa *et al.* (PACS-CS Collaboration), *Phys.Rev.* **D87**, 094512 (2013), [arXiv:1301.4743 \[hep-lat\]](#).
- [15] H. Na and S. Gottlieb, *PoS LATTICE2008*, 119 (2008), [arXiv:0812.1235 \[hep-lat\]](#).
- [16] C. Albertus, E. Hernandez, J. Nieves, and J. Verde-Velasco, *Eur.Phys.J.* **A32**, 183 (2007), [arXiv:hep-ph/0610030 \[hep-ph\]](#).
- [17] M. Moinester *et al.* (SELEX Collaboration), *Czech.J.Phys.* **53**, B201 (2003), [arXiv:hep-ex/0212029 \[hep-ex\]](#).
- [18] B. Aubert *et al.* (BaBar Collaboration), *Phys.Rev.* **D74**, 011103 (2006), [arXiv:hep-ex/0605075 \[hep-ex\]](#).
- [19] R. Chistov *et al.* (BELLE Collaboration), *Phys.Rev.Lett.* **97**, 162001 (2006), [arXiv:hep-ex/0606051 \[hep-ex\]](#).
- [20] S. Ogilvy (LHCb), *Proceedings, 6th International Workshop on Charm Physics (Charm 2013)* (2013), [arXiv:1312.1601 \[hep-ex\]](#).

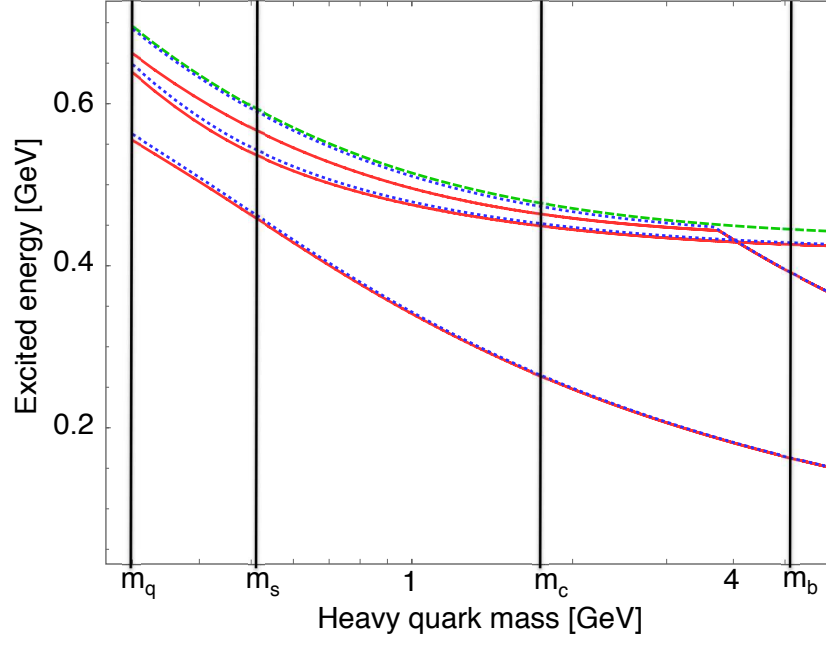


FIG. 10: Heavy quark mass dependence of excited energy of first state, second state and third state for $1/2^-$ (red solid line), $3/2^-$ (blue dotted line), $5/2^-$ (green dashed line) of Ξ_{QQ} .

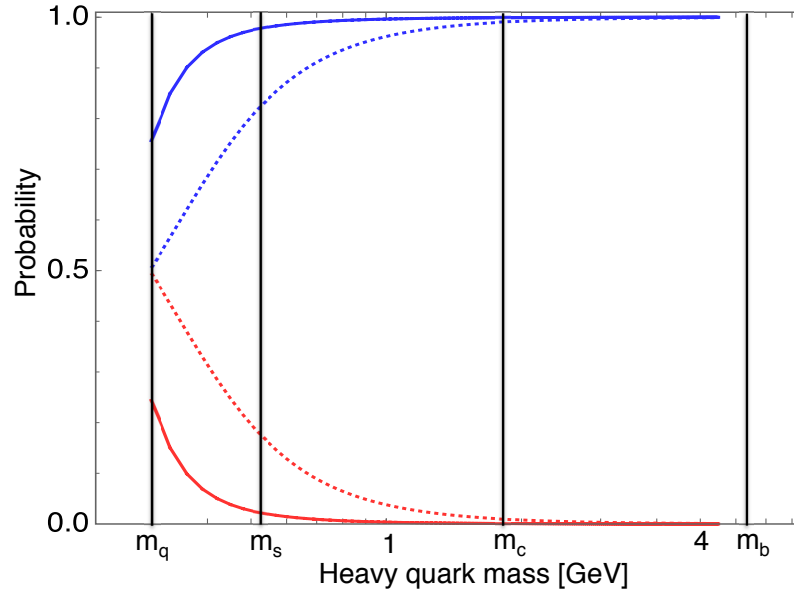


FIG. 11: The probability of λ mode (blue line) and ρ mode (red line) of $\frac{1}{2}^-$ for Σ_Q (dotted line), Λ_Q (Solid line).

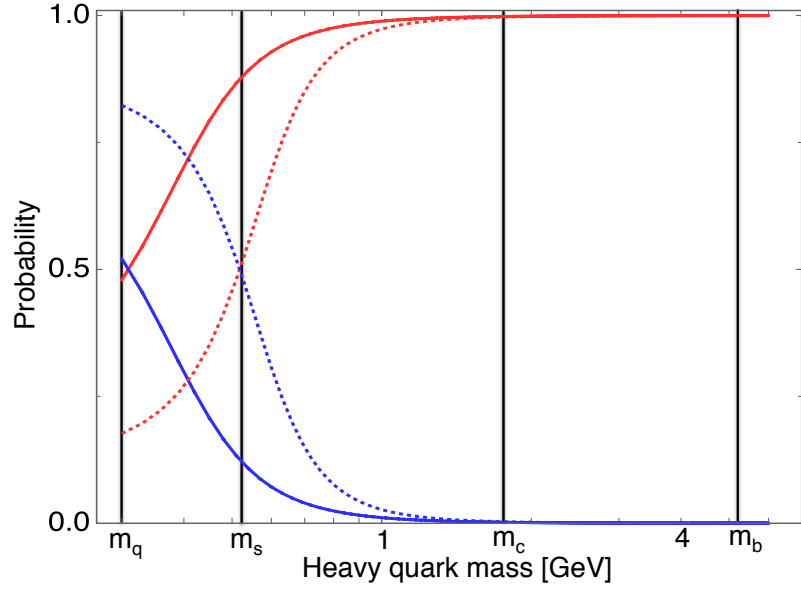


FIG. 12: The probability of λ mode (blue line) and ρ mode (red line) of $\frac{1}{2}^-$ for Ξ_{QQ} (Solid line) and Ω_{QQ} (dotted line).

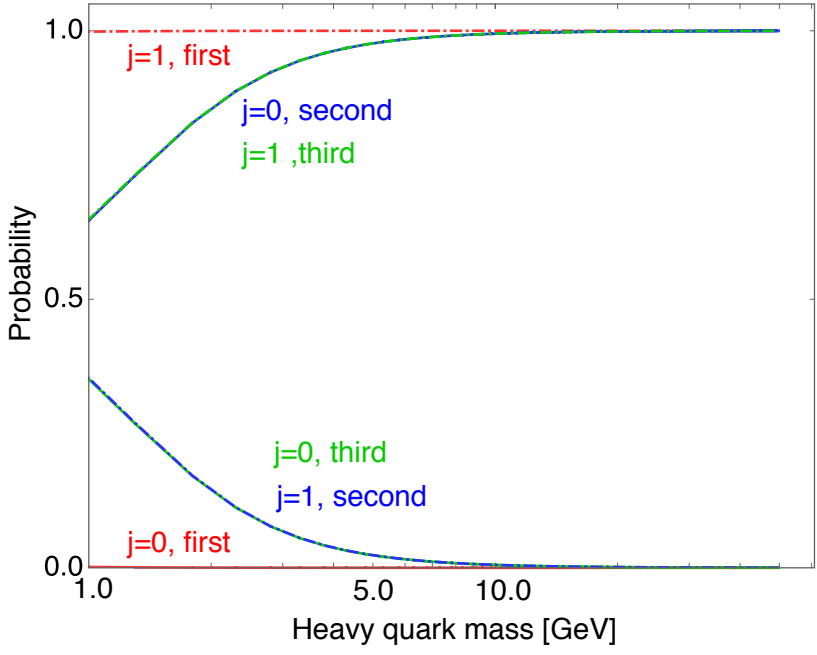


FIG. 13: The probabilities of $j=0$ (Solid line) and $j=1$ (Chain line) for $\Lambda(1/2^-)$. Red, blue, green lines show the first state, second state and third state respectively.

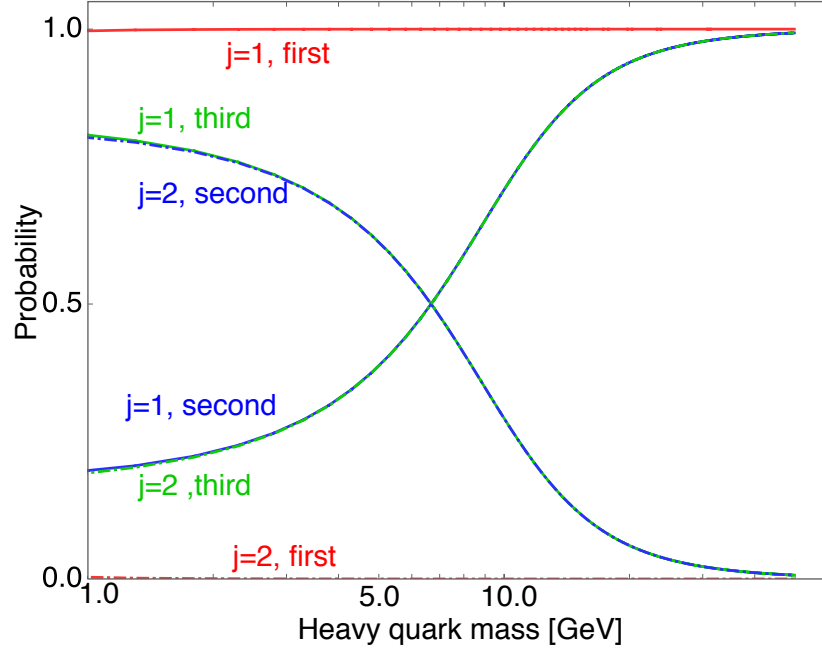


FIG. 14: The probabilities of $j=1$ (Solid line) and $j=2$ (Chain line) for $\Lambda(3/2^-)$. Red, blue, green lines show the first state, second state and third state respectively.

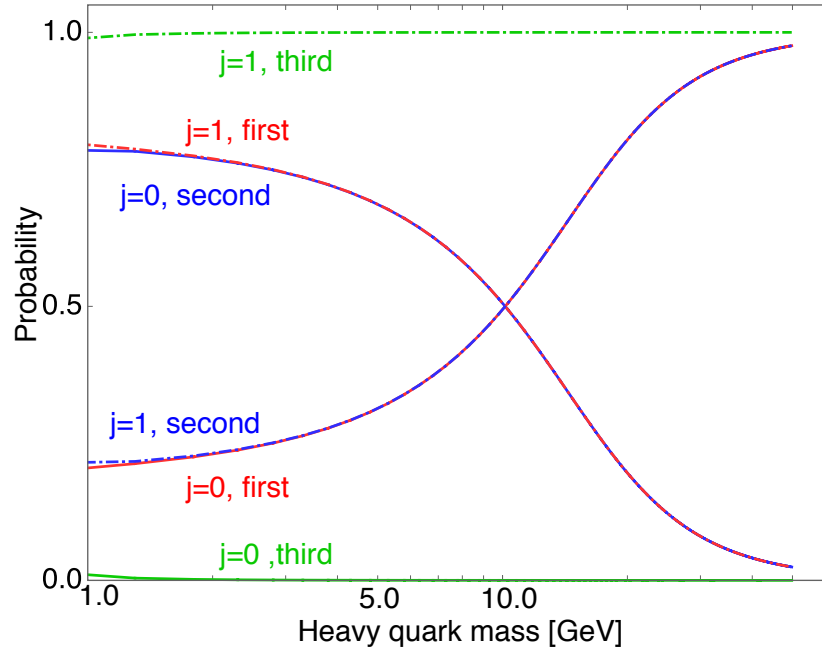


FIG. 15: The probabilities of $j=0$ (Solid line) and $j=1$ (Chain line) for $\Sigma(1/2^-)$. Red, blue, green lines show the first state, second state and third state respectively.

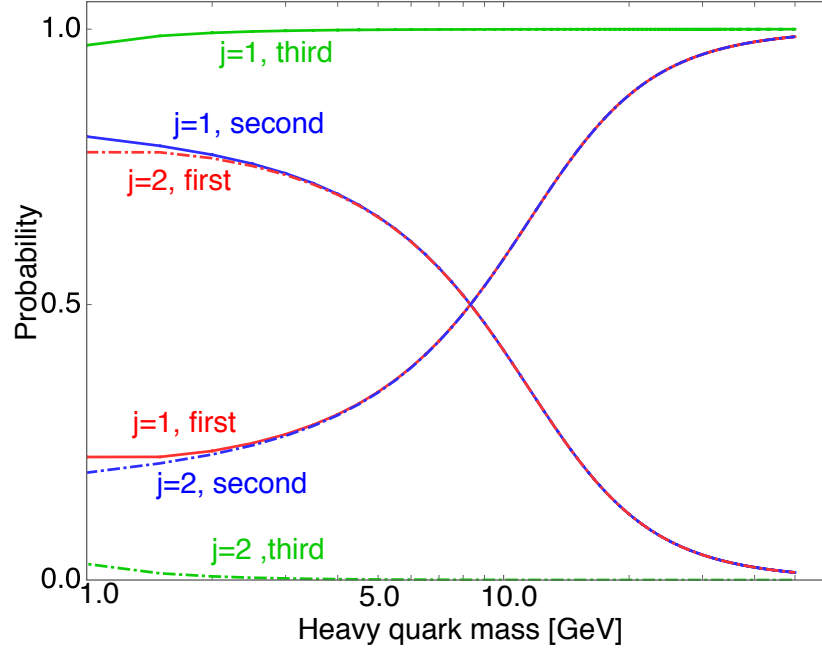


FIG. 16: The probabilities of $j=1$ (Solid line) and $j=2$ (Chain line) for $\Sigma(3/2^-)$. Red, blue, green lines show the first state, second state and third state respectively.

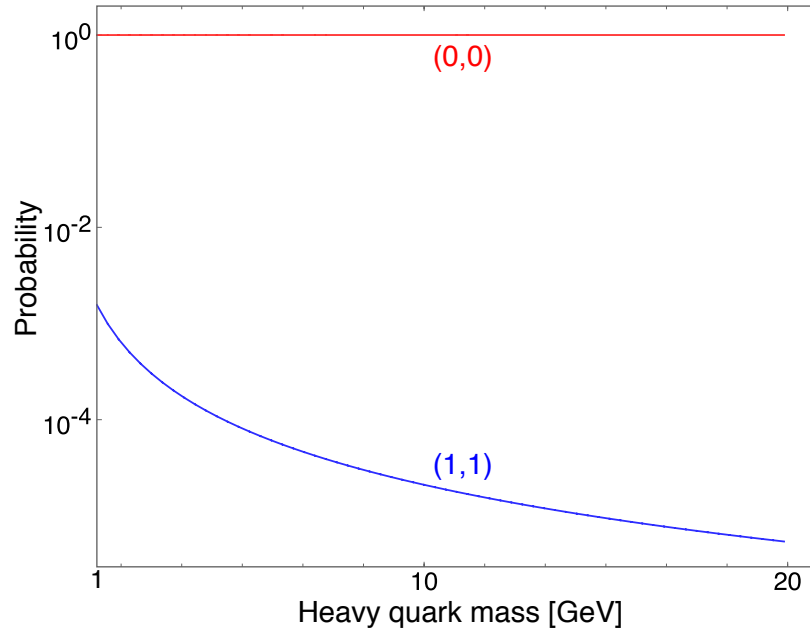


FIG. 17: The heavy quark mass dependence of the probabilities of the S-wave (0,0) component (Red line) and (1,1) component (blue line) for $\Lambda(1/2_1^+)$.

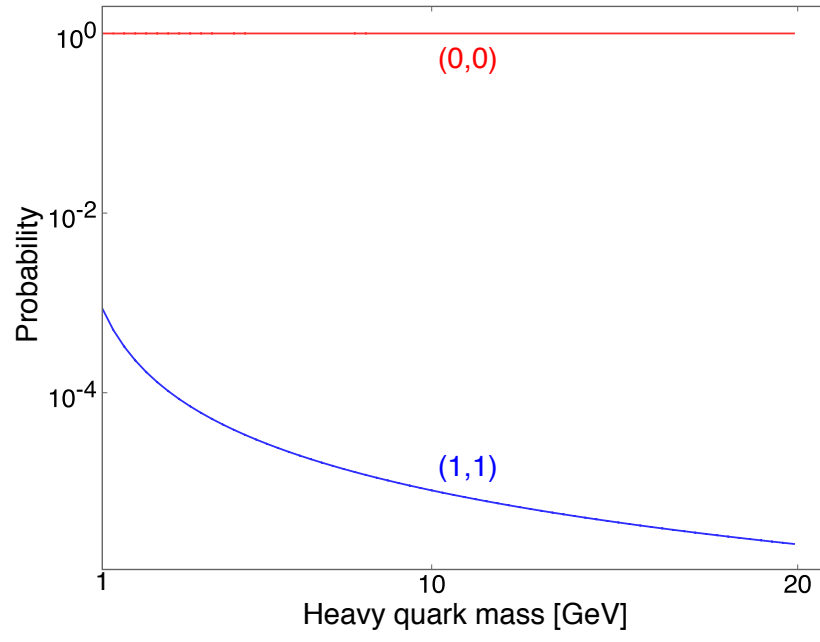


FIG. 18: The heavy quark mass dependences of the probabilities of the S-wave (0,0) component (Red line) and (1,1) component (blue line) for $\Lambda(1/2_2^+)$.

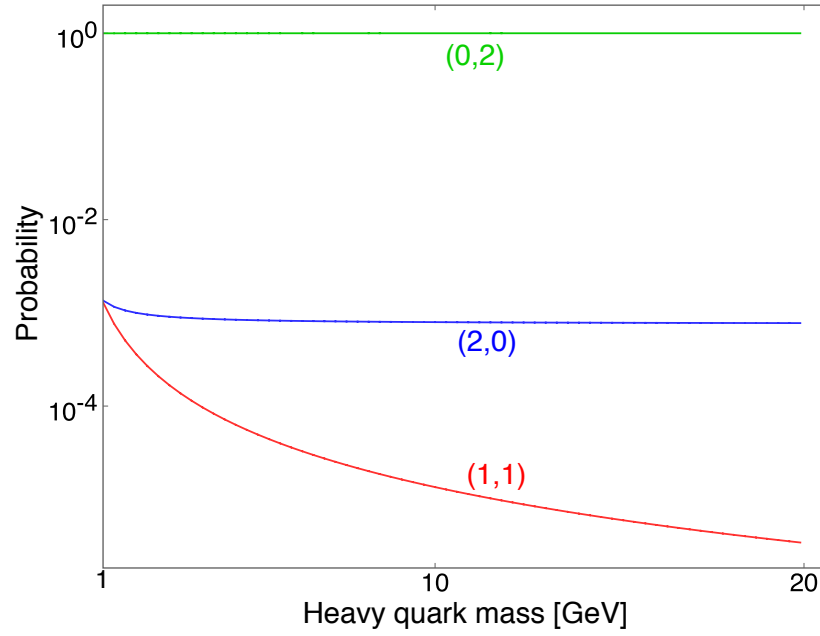


FIG. 19: The heavy quark mass dependences of the probabilities of (1,1) component (red line), (2,0) component (blue line) and (0,2) component (green line) for $\Lambda(3/2_1^+)$.

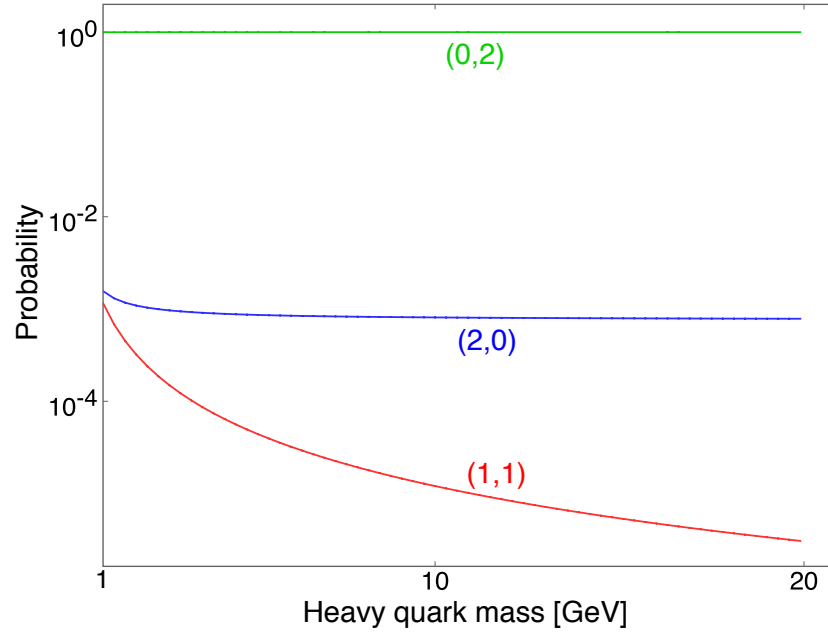


FIG. 20: The heavy quark mass dependences of the probabilities of (1,1) component (red line), (2,0) component (blue line) and (0,2) component (green line) for $\Lambda(5/2_1^+)$.

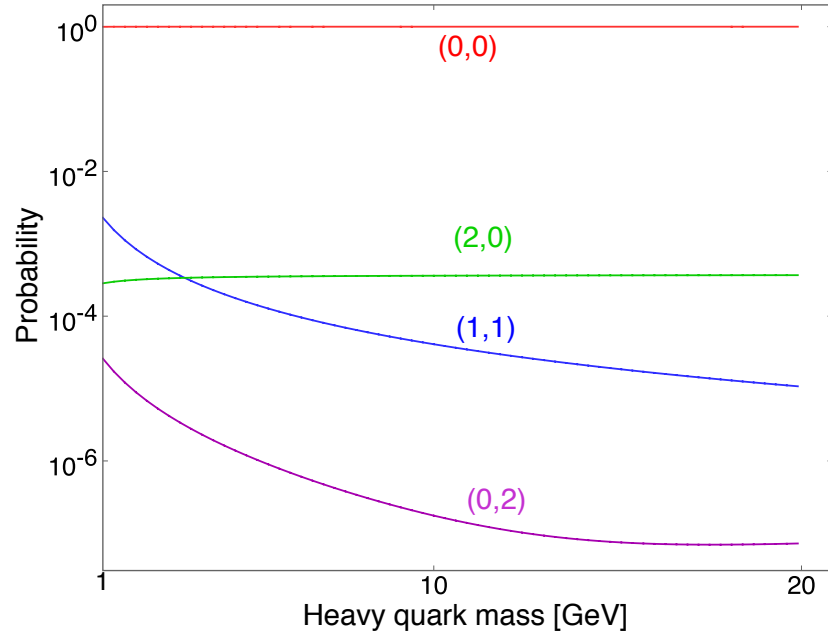


FIG. 21: The heavy quark mass dependences of the probabilities of the S-wave (0,0) component (red line), (1,1) component (blue line), (2,0) component (green line) and (0,2) component (violet line) for $\Sigma(1/2_1^+)$.

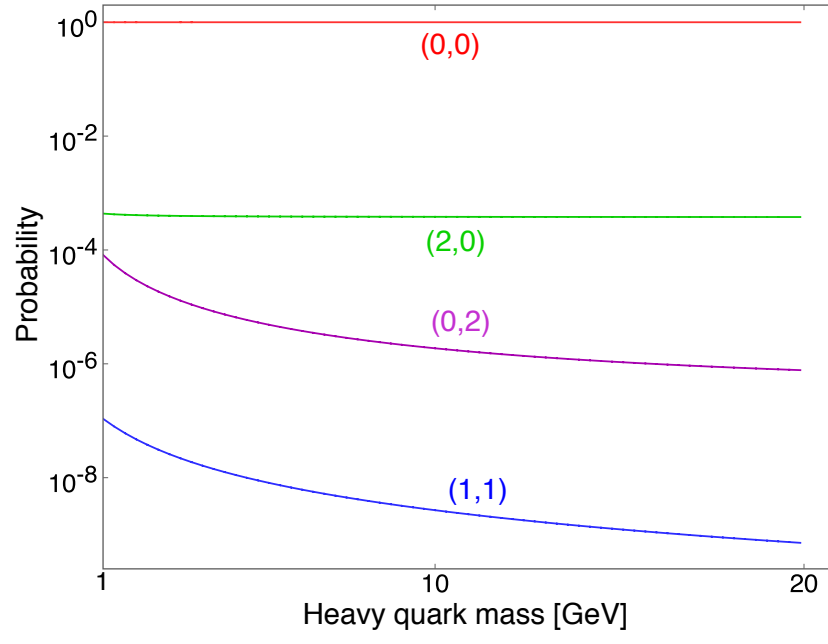


FIG. 22: The heavy quark mass dependences of the probabilities of the S-wave ($l=0, L=0$) component (red line), $(1,1)$ component (blue line), $(2,0)$ component (green line) and $(0,2)$ component (violet line) for $\Sigma(3/2_1^+)$.